NUREG/IA-0146

International Agreement Report

Implementation and Assessment of Improved Models and Options in TRAC-BF1

Prepared by
G. Th. Analytis

Laboratory for Thermal Hydraulics
Paul Scherrer Institute
CH-5232 Villigen PSI
Switzerland

Office of Nuclear Regulatory Research
U.S. Nuclear Regulatory Commission
Washington, DC 20555–0001

October 1998

Prepared as part of
The Agreement on Research Participation and Technical Exchange
under the International Code Application and Maintenance Program (CAMP)

Published by
U.S. Nuclear Regulatory Commission

AVAILABILITY NOTICE

Availability of Reference Materials Cited in NRC Publications

NRC publications in the NUREG series, NRC regulations, and *Title 10, Energy,* of the *Code of Federal Regulations,* may be purchased from one of the following sources:

1. The Superintendent of Documents
   U.S. Government Printing Office
   P.O. Box 37082
   Washington, DC 20402–9328
   <http://www.access.gpo.gov/su_docs>
   202–512–1800

2. The National Technical Information Service
   Springfield, VA 22161–0002
   <http://www.ntis.gov/ordernow>
   703–487–4650

The NUREG series comprises (1) technical and administrative reports, including those prepared for international agreements, (2) brochures, (3) proceedings of conferences and workshops, (4) adjudications and other issuances of the Commission and Atomic Safety and Licensing Boards, and (5) books.

A single copy of each NRC draft report is available free, to the extent of supply, upon written request as follows:

Address: Office of the Chief Information Officer
Reproduction and Distribution
Services Section
U.S. Nuclear Regulatory Commission
Washington, DC 20555–0001
E–mail: <GRW1@NRC.GOV>
Facsimile: 301–415–2289

A portion of NRC regulatory and technical information is available at NRC's World Wide Web site:

<http://www.nrc.gov>

All NRC documents released to the public are available for inspection or copying for a fee, in paper, microfiche, or, in some cases, diskette, from the Public Document Room (PDR):

NRC Public Document Room
2121 L Street, N.W., Lower Level
Washington, DC 20555–0001
<http://www.nrc.gov/NRC/PDR/pdr1.htm>
1–800–397–4209 or locally 202–634–3273

Microfiche of most NRC documents made publicly available since January 1981 may be found in the Local Public Document Rooms (LPDRs) located in the vicinity of nuclear power plants. The locations of the LPDRs may be obtained from the PDR (see previous paragraph) or through:

<http://www.nrc.gov/NRC/NUREGS/SR1350/V9/lpdr/html>

Publicly released documents include, to name a few, NUREG-series reports; *Federal Register* notices; applicant, licensee, and vendor documents and correspondence; NRC correspondence and internal memoranda; bulletins and information notices; inspection and investigation reports; licensee event reports; and Commission papers and their attachments.

Documents available from public and special technical libraries include all open literature items, such as books, journal articles, and transactions, *Federal Register* notices, Federal and State legislation, and congressional reports. Such documents as theses, dissertations, foreign reports and translations, and non-NRC conference proceedings may be purchased from their sponsoring organization.

Copies of industry codes and standards used in a substantive manner in the NRC regulatory process are maintained at the NRC Library, Two White Flint North, 11545 Rockville Pike, Rockville, MD 20852–2738. These standards are available in the library for reference use by the public. Codes and standards are usually copyrighted and may be purchased from the originating organization or, if they are American National Standards, from—

American National Standards Institute
11 West 42nd Street
New York, NY 10036–8002
<http://www.ansi.org>
212–642–4900

NUREG/IA-0146

International Agreement Report

Implementation and Assessment of Improved Models and Options in TRAC-BF1

Prepared by
G. Th. Analytis

Laboratory for Thermal Hydraulics
Paul Scherrer Institute
CH-5232 Villigen PSI
Switzerland

Office of Nuclear Regulatory Research
U.S. Nuclear Regulatory Commission
Washington, DC 20555–0001

October 1998

Prepared as part of
The Agreement on Research Participation and Technical Exchange
under the International Code Application and Maintenance Program (CAMP)

Published by
U.S. Nuclear Regulatory Commission

ABSTRACT

A summary of modifications and options introduced in TRAC-BF1 is presented and is shown that the predicting capabilities of the modified version of the code are greatly improved. These changes include the introduction of a different heat transfer package during reflooding, the implementation of a simple single-phase limit procedure for forcing the two phases to acquire the same velocity if one phase disappears, a close assessment of the annular flow interfacial shear correlation, implementation of a simple radiation model which seems to alleviate some numerical-oscillations problems induced by the existing highly complex model. Furthermore, different options were introduced and tested like upwinding some terms of the momentum equations (which seems to solve a number of problems reported in the past), the second upwind scheme for the convective terms of the phasic momentum equations and the implementation and assessment of a completely different annular flow interfacial shear correlation.

The modified TRAC-BF1 is assessed against some bottom-flooding separate-effect experiments, a "benchmark" top flooding simulation as well as against the TLTA test Nr. 6423. In the process of this task, the different options are assessed and discussed and is shown that the predictions of the modified code are physically sound and close to the measurements, while almost all the predicted variables are free of unphysical spurious oscillations. The modifications introduced solve a number of problems associated with the frozen version of the code and result in a version which can be confidently used for LB-LOCA analyses.

CONTENTS

Figures

Figures (Cont)

1 INTRODUCTION

TRAC-BF1 is a best-estimate transient analysis thermohydraulics code for BWRs and its original development at Idaho National Engineering Laboratories started at the early 80s in collaboration with General Electric (GE). The original versions of the code were TRAC-BD1 and TRAC-BD1/MOD1 and were both using the semi-implicit solution scheme for the hydraulic equations. TRAC-BF1 is an improved version of the aforementioned previous versions and among a number of improvements which make the code both physically more sound and numerically more robust, is the Courant - violating numerics for the 1-Dimensional (1D) components. For a more detailed reading of the different models in the code as well as the numerical solution techniques, the interested reader is referred to Taylor et al., (1984) and Borowski and Wade (1992a,b).

A systematic assessment of some models in TRAC-BF1 started at PSI in 1990 and one of the areas to which attention was paid was the modelling of heat transfer during reflooding. The code version used for this work (and also used for the work to be reported here) was obtained from INEL in the summer of 1990 and is the UNICOS 5.1 version named **1U5test G2W2**. We shall refer to this as the **frozen version of the code**. Since the models which we have changed and on which we shall elaborate in this work are still the same in the present frozen version of the code, we shall still be referring to the unmodified version as the frozen version, although we shall be actually referring to an older version than the one on which the term **frozen** would be appropriate.

In TRAC-BF1, the code developers had already adopted the Bestion interfacial shear correlation (Bestion, 1985) for bubbly/slug flow in rod bundles as recommended in the past (Analytis, 1995) who showed that the corresponding model in the code is not suitable for rod bundles. In trying to assess the code's capabilities to model reflooding, a number of separate-effect bottom flooding tests at the heater rod bundle NEPTUN test facility (Grütter et al., 1980) at PSI were analysed and a number of interesting observations were made which resulted in a set of model changes (Analytis, 1992). One of the major model changes implemented in the code was a special wall-to-liquid heat transfer package activated during reflooding which expresses the heat transfer coefficient (HTC) by an empirical correlation exhibiting its experimentally observed strong dependence as a function of the distance from the quench front(s) (QF(s)) as in the French code CATHARE (Juhel, 1984; Bestion, 1991). Furthermore, an upwinding scheme of some terms of the finite-differenced phasic momentum equations was implemented in the code (Analytis and Coddington, 1992), the aim of which was to solve some problems arising from the cell-centered way that these terms were finite-differenced in the frozen version of the code and in particular, the way they were used in the wall shear modelling. This was successfully accomplished. The modified version of the code was also used to analyse a hypothetical LB-LOCA in a BWR-4 operating at 110% power and under the assumption of limited ECCS (Analytis, 1995).

In this work, we shall summarise all the model changes and options we have implemented in TRAC-BF1. Some of these changes are a little different to the ones reported in the past (Analytis, 1992), while some others we have found not necessary (eg the reduction of the interfacial heat transfer from the vapour to the droplets) . Additionally, we have

now implemented some new changes and options not implemented earlier in the code (Analytis, 1992; Analytis and Coddington, 1992), which nevertheless we found helpful and necessary. After discussing in some details all these modifications and options in section 2, in section 3, we shall analyse a number of bottom flooding experiments in the NEPTUN test facility (which is a heater rod bundle) both with the frozen and modified version of the code and discuss the differences between them as well as the effect of the annular flow interfacial shear correlation on the predictions. Additionally, we shall analyse a top flooding benchmark test with different versions of the code and we shall look in more detail on the effect of different interfacial and wall shear models on the code predictions. Furthermore, we shall report on the analysis of the TLTA test Nr. 6423 with different versions of the code. Finally, in section 4, we shall conclude this work by making some recommendations.

2 SUMMARY OF MODIFICATIONS AND OPTIONS IN TRAC-BF1

We shall now outline the code modifications and model changes we have implemented in TRAC-BF1. Some of these changes are a little different to the ones reported in the past (Analytis, 1992); additionally, a number of additional options have been added in the code which we shall summarise.

(a) The main modification implemented in TRAC-BF1 was that during reflooding, a special wall-to-liquid heat transfer package is used, similar to the one in an older version of the French code CATHARE (Juhel, 1984; Bestion, 1991). In TRAC-BF1, as in other existing thermohydraulic system codes like RELAP5/MOD3 (Carlson et al., 1990), there is only one post-CHF wall-to-liquid heat transfer package independently of the physical process that is supposed to be modelled. This package is based on modelling the wall-to-liquid film boiling HTC in subroutine **HTCOR** by (Taylor et al., 1984; Borowski and Wade, 1992a)

$$h_{wl(FB)} = (1 - \alpha) h_{(mod,BR)} \tag{2.1}$$

where $h_{mod,BR}$ is the **modified** Bromley correlation and α is the void fraction. This wall-to-liquid HTC is used if the wall temperature T_w is greater than a minimum film boiling temperature T_{MIN} which in the code is given either by the homogeneous nucleation temperature, or by the Shumway correlation. If now the T_w is lower than T_{MIN} but greater than the wall temperature T_{CHF} at the critical heat flux, transition boiling is assumed to occur, and the code uses the Bjornard quadratic interpolation between the CHF point and the film-boiling wall-to-liquid HTC $h_{wl(FB)}$) in the usual way

$$h_{wl(TB)} = (1 - \Gamma)\, h_{wl(FB)} + \Gamma \frac{q_{CHF}}{T_w - T_l} \tag{2.2a}$$

where

$$\Gamma = \left(\frac{T_w - T_{MIN}}{T_{CHF} - T_{MIN}} \right)^2 \qquad (2.2b)$$

and all the symbols have their usual meaning.

Clearly, as is well-known, the aforementioned approach does not take into account the experimentally established fact that during reflooding, there is a strong dependence (in fact, enhancement) of the HTC in the vicinity of the QF, far above the values one would get in non-reflooding situations. Hence, while we only introduced the simple radiation model described below in **HTCOR** (notice that this subroutine is also called by the subroutine **CHNQ** which activates the fine-mesh for the channel-wall), we added the subroutine **HTCOR1** which is called only if the reflooding is activated and the component is the core. In this subroutine, in addition to the aforementioned radiation model, we implemented the simple empirical wall-to-liquid heat transfer correlation which is similar to the one in an older version of the French code CATHARE and reads (Juhel, 1984)

$$h_{wl(FB)} = max \left\{ (1400 - 1880\, \Delta z_{QF}) \right.$$
$$\left. min\,(1 - \alpha,\, 0.5),\, 0 \right\} + h_{BR} \sqrt{1 - \alpha} \qquad (2.3)$$

where Δz_{QF} is the distance from the top or bottom quench-fronts (QFs) and h_{BR} is the original Bromley correlation with $h_{BR} \sim (\Delta z_{QF})^{-0.25}$. The same wall-to-liquid HTC is assumed independently of whether we are in the vicinity of the bottom or top QFs. Here, we should point out that since during reflooding, we hope that the present approach will actually predict the "knee temperature" as being the temperature of the rod at this elevation when the QF arrives there (as is physically the case), if the aforementioned reflooding heat transfer logic is activated, we have assumed the actual homogeneous nucleation temperature as the minimum film boiling temperature rather than trying to obtain this temperature from a correlation as is done in the code if one sets in the input ITMIN=1, by which the Shumway correlation is chosen as the "knee temperature". We shall see in the next section that if this option is chosen, due to the fact that the Shumway correlation predicts a "knee temperature" higher than the homogeneous nucleation temperature, one is forcing unphysically the different rod nodes to quench at a relatively high temperature independently of whether the QF is in the vicinity of the node or not. As a result of this, large oscillations may appear in the calculated quantities like velocities, void fractions etc. In this work, in the analysis of separate-effect bottom flooding experiments, we are not allowing any top quenching since we are preventing the code from going to transition boiling (and subsequently, to nucleate boiling) if the distance from the bottom QF is greater than 0.1 m. For the general case, this is clearly not so since if there is no CCFL, during spray cooling, there will certainly be a film created at the top of the rods (and hence, a top QF) which will start propagating downwards.

We should point out here that during reflooding, we have implemented a similar wall-to-liquid heat transfer model in RELAP5/MOD3 (Analytis, 1995, 1996). There, the

model is a little different in as far as in addition to defining a HTC by eq. (2.3), the final HTC used in the film-boiling regime during reflooding is given by the maximum of eq. (2.3) and the one of Forslund-Rohsenow for contact heat transfer between the hot walls and the droplets. We think that a number of differences between the constitutive equations of the two codes may be responsible for this difference (eg the interfacial shear package is quite different in RELAP5/MOD3 when compared to the one of TRAC-BF1).

(b) There are different CHF options in the code, one of them being the Biasi correlation. In relation to reflooding, we have already shown in relation to RELAP5/MOD3 (Analytis, 1995, 1996) that although in reality the actual value of the CHF is not of great importance, the way it is used in the wall heat transfer package can excite numerical oscillations if such oscillations exist on the CHF. A CHF correlation which is a very simple mathematical expression and has been shown not to exhibit any oscillating behaviour is the simple modified Zuber correlation and during reflooding, this was the one used in RELAP5/MOD2 and MOD2.5 (Ransom et al., 1985). Hence, if the reflooding is on, we use the following CHF correlation:

$$q_{CHF} = q_{(CHF,Zuber)}\, max\left(1, \left(\frac{G}{G_{ref}}\right)^{0.333}\right) \tag{2.4}$$

where G is the total mass-flux and $G_{ref} = 67.8\ kg/m^2 s$. As we have already mentioned before, while the actual value of the CHF is of the utmost importance in cases that the prediction of the dry-out point is required, in the case of reflooding, it is not so important.

(c) The drift-flux interfacial shear package in the code (subroutine **FRCIF**) was derived (Andersen et al., 1983), based on the work by Ishii (1977) who computed the drift-flux parameters V_{gj} and C_0 for different flow regimes. For annular flow, the V_{gj} and C_0 obtained by Ishii (1977) were based on the Wallis interfacial shear correlation and the expressions derived by Andersen and used in TRAC-BF1 (Taylor et al., 1984, Borowski and Wade, 1992a, 1992b) are

$$C_0 = 1 + \frac{(1 - \alpha)\,(1 - e)}{(\alpha + a)} \tag{2.5a}$$

where

$$a = \sqrt{\frac{1 + 75\,(1 - \alpha)}{\sqrt{\alpha}}}\sqrt{\frac{\rho_g}{\rho_l}} \tag{2.5b}$$

e is the fraction of the entrained liquid and is calculated as in TRAC-BF1 in the following way:

$$e = max\,(\,(xe - 0.03), 0.0)/\sqrt{1 + (0.1 + xe)^2} \tag{2.5c}$$

where

$$xe = 10^{-6}\sqrt{(\sqrt{j_g^{*\,10}\, D^{*5}\, Re_l})}\,. \tag{2.5d}$$

$$Re_l = |G_l|\, D_H \,/\, \mu_l\,, \tag{2.5e}$$

$$G_l = (1 - \alpha)\,\rho_l\,V_l\,, \tag{2.5f}$$

$$D^* = D_H\,\sqrt{9.81\,(\rho_l - \rho_g)\,/\,\sigma}\,, \tag{2.5g}$$

$$j_g^* = |j_g|\,/\,\sqrt{\sqrt{\sigma\,9.81\,(\rho_l - \rho_g)\,(\rho_g\,/\,(\rho_l - \rho_g))^{.66666}\,/\,\rho_g^2}}\,, \tag{2.5h}$$

and

$$j_g = \alpha\,V_g\,. \tag{2.5i}$$

Then, we shall have

$$C_{IO} = \frac{0.015\,\rho_l\,\alpha\,(a + \alpha)^2}{D_H} \tag{2.6a}$$

and the interfacial shear per unit volume will be

$$f_i = \frac{0.015\,\rho_l\,\alpha\,(a + \alpha)^2}{D_H}\,(C_1 V_g - C_0 V_l)^2. \tag{2.6b}$$

where

$$C_1 = \frac{1 - \alpha\,C_0}{1 - \alpha}, \tag{2.6c}$$

Notice that the aforementioned annular flow interfacial shear correlation it was assumed that the continuous phase is the liquid and hence, the liquid density ρ_l appears as multiplier. This makes the interfacial shear up to three orders of magnitude higher than the one of Wallis which is based on the assumption that the continuous phase is the vapour and reads

$$f_i = \frac{0.005\,\rho_g}{D_H}\left(1 + 75(1 - \alpha)(1 - e)\right)\,(V_g - V_l)^2. \tag{2.7a}$$

(In the Wallis correlation, $C_0 = C_1 = 1$). As a matter of fact, the drift-flux parameters V_{gj} and C_0 computed by Ishii for annular flow were based on this correlation; should the assumption had been made that in annular flow, the continuous phase is the vapour, equation (2.6b) would read

$$f_i = \frac{0.015\,\rho_g\,\alpha\,(a + \alpha)^2}{D_H}\,(C_1 V_g - C_0 V_l)^2. \tag{2.7b}$$

and this is "equivalent" to the Wallis correlation Hence, by changing the ρ_l to ρ_g in the annular flow interfacial shear correlation in TRAC-BF1, one should get results equivalent to the ones obtained by using explicitly the aforementioned Wallis correlation. In the course of this work, we have realized that although for bottom flooding, if the code assumes annular flow, the interfacial shear correlation as it stands in the code is too high and always results in excessive liquid carry-over, if the water is entering from the top, it gives quite reasonable results and can even "predict" a kind of falling film. The opposite is true if the continuous phase is assumed to be the vapour (as in the Wallis correlation); then, the interfacial shear is sufficiently small to prevent excessive carry-over during bottom flooding but in contrast, if the water enters from the top, one obtains rather unphysical results, the entering liquid is pushed to the bottom and no film is created at the top. Recently *

* P. Coddington, Private communication (1996)

it was suggested that this pathological behaviour may be due to the particular form of the wall shear model used in the code (which is also responsible for the pathological behaviour reported in the past (Analytis and Coddington, 1992), which led us to the upwinding of some terms of the momentum equations) and attempts were made to investigate this possibility. Under item (j) below, we shall further report on this problem and show that if one uses a wall shear model like the one of TRAC-PF1 (Liles et al., 1986; Gao and Leslie, 1989) which is not based on the total pressure-drop (hence requiring subsequent partitioning of the wall shear between the two phases) but rather defines the wall friction individually for each phase (or if one tries somehow not to "weight" the wall shear between the liquid and the vapour with the liquid fraction), most of the aforementioned problems are solved.

Finally, in the code, the following values of C_{IO} are used in the phasic momentum equations:

If $1 - \alpha < 0.1$,

$$C_{IO} = 10\, C_{IO}\, (1 - \alpha). \tag{2.8a}$$

If $1 - e < 0.1$,

$$C_{IO} = 10\, C_{IO}. \tag{2.8b}$$

If $1 - e > 0.1$,

$$C_{IO} = \frac{C_{IO}}{1 - e}. \tag{2.8c}$$

As an option, we introduced in the code the original Wallis correlation (which, in a way, is equivalent to changing ρ_l to ρ_g in the correlation in TRAC-BF1).

(d) As an additional option, we implemented in the code the Bharathan annular flow interfacial shear correlation used in RELAP5/MOD2, the interfacial shear coefficient of which reads:

$$C_{IO} = S_{ann}\, \rho_g \left(0.0025 + 0.1375\, 10.0^{(9.07\, R^*)}\, F^{(1.63 + 4.74\, R_D^*)} \right) \tag{2.9}$$

where the symbols are defined as follows:

$$S_{ann} = \frac{6.1192775\, \sqrt{R_D^*}\, \alpha_{gs}}{D_H}, \tag{2.10a}$$

$$F = max(10^{-8}, 0.5\, (1 - \alpha_{gs})\, D^*), \tag{2.10b}$$

$$R^* = min\left(30, \frac{1}{D^*}\right), \tag{2.10c}$$

$$R_D^* = \sqrt{\sqrt{\alpha_b}}, \tag{2.10d}$$

D^* is defined by (2.5g) and

$$\alpha_b = max(0,\, (1 - \alpha)\, V_{gbb}), \tag{2.10e}$$

$$\alpha_{gs} = \sqrt{1 - \alpha_b} \qquad (2.10f)$$

where

$$V_{gbb} = e^{-S_c}\, max\left(0,\ \left(1 - 10^{-4}\sqrt{\sqrt{\frac{|V_l\,(1-\alpha)\,\rho_l\,D_H|}{\mu_l}}}\right)\right) \qquad (2.10g)$$

and

$$V_{crit} = 2.5\sqrt{\frac{\sqrt{\sigma\,(\rho_l - \rho_g)}}{\rho_g}} \qquad (2.10h)$$

where

$$S_c = 4\,10^{-5}\left(\frac{\alpha\,V_g}{V_{crit}}\right)^6. \qquad (2.10i)$$

The distribution coefficients C_o and C_1 in the interfacial shear per unit volume f_i are equal to 1 and $\alpha_d = 10^{-7}$. The employment of this correlation during the analysis of different tests alleviated many problems encountered with the aforementioned other two correlations. This we implemented in a new subroutine called **FRCIFR** which is called if this option is required.

(e) The drift-flux coefficients C_0 and C_1 are modified in the interfacial shear subroutine **FRCIF** if $V_l < 0$ and $V_g > 0$; if this is the case, CCFL is assumed in **FRCIF**, even if the actual CCFL flag in the code (**ICCFL**) is switched-off. Though, one can easily have a situation in which at one node, $V_l < 0$ and $V_g > 0$ (for example, during bottom flooding), without having CCFL, but simply because the droplet is too heavy to be lifted by the vapour and falls back. Hence, we removed the modifications of C_0 and C_1 which were responsible for some numerical oscillations, since clearly, one can have at one time step $V_l < 0$ and at the next, $V_l > 0$. Though, these modifications are still activated but now only if for that node $ICCFL \neq 0$. To achieve this, the flag $ICCFL$ is made an argument of the subroutines **FRCIF** and **FRCIFR**.

(f) In order to let the liquid velocity V_l approach the vapour velocity V_g as $\alpha -> 1$, in a previous work (Analytis, 1992), we have utilised an approach similar to the one used in the old version of the code, TRAC-BD1. In this work, we use a different approach and assume that the interfacial shear calculated by the code is valid up to $\alpha = 0.9999999999$; for $\alpha > 0.99999999999$, a value given by $\alpha(1-\alpha)10^{20}$ was assumed while between the two limits, we used an interpolation. We did this modification both for the 1D and 3D vessel component. For doing this, some limits defined in the solution subroutines **TF1E** and **TF3E** of the 1D and 3D momentum equations had to be modified. This approach is different to the one reported by Analytis (1992).

(g) Similarly to other system thermohydraulic transient analysis codes like RELAP5, in TRAC-BF1, in the semi-implicit numerical solution scheme, (subroutine **TF1E**), for each edge of a computational cell and for each time-step, after linearising the interfacial (and wall) shear terms (for more details, see (j) below), the 2 phasic discretized momentum equations are solved as a system of 2 linear algebraic equations

with the new phasic velocities at the edges $(k + \frac{1}{2})$ of the computational volumes as unknowns, e.g.

$$\begin{pmatrix} M_{11} & M_{12} \\ \\ M_{21} & M_{22} \end{pmatrix} \begin{pmatrix} V^{n+1}_{g,\, k+\frac{1}{2}} \\ \\ V^{n+1}_{l,\, k+\frac{1}{2}} \end{pmatrix} = \begin{pmatrix} R^n_g \\ \\ R^n_l \end{pmatrix} \tag{2.11a}$$

where a superscript indicates the time-step and

$$M_{ij} = f\Bigg(....., \frac{1}{\overline{(\alpha_p\, \rho_p)}^{n}_{k+\frac{1}{2}}}, \frac{C_{IO}\,(\tilde{\alpha}^{n}_{g,\, k+\frac{1}{2}})}{\overline{(\alpha_p\, \rho_p)}^{n}_{k+\frac{1}{2}}}, \left(f_w\right)^n_{p,\, k+\frac{1}{2}}, V^n_{p,\, k+\frac{1}{2}} ... \Bigg) \tag{2.11b}$$

is a function of a number of old-time variables. The subscript "p" refers to the phase p (g or l) while f_w is the wall friction, and $C_{IO}(\tilde{\alpha}^{n}_{g,\, k+\frac{1}{2}})$ the flow-regime dependent interfacial shear coefficient which depends on the junction void fraction $\tilde{\alpha}^{n}_{g,\, k+\frac{1}{2}}$ while a twiddle over indicates that is upwinded. An upwinded phasic quantity $\tilde{Y}^{n}_{p,\, k+\frac{1}{2}}$ is defined by

$$\tilde{Y}^{n}_{p,\, k+\frac{1}{2}} = (WP)\,(Y_p)^n_k + (WP1)\,(Y_p)^n_{k+1} \tag{2.12a}$$

where

$$(WP) = \begin{cases} 1 & V^n_{p,\, k+\frac{1}{2}} > 0 \\ \\ 0 & V^n_{p,\, k+\frac{1}{2}} \leq 0 \end{cases} \tag{2.12b}$$

$$(WP1) = 1 - (WP). \tag{2.12c}$$

$(Y_p)^n_k$ and $(Y_p)^n_{k+1}$ are the cell-centred phasic quantities up-stream and down-stream the junction $(k + \frac{1}{2})$, respectively. Finally, in eq.(2.11a), R^n_p are

$$R^n_p = f\Bigg(....., \frac{1}{\overline{(\alpha_p\, \rho_p)}^{n}_{k+\frac{1}{2}}}, \frac{P^{n+1}_{k+1} - P^n_k}{\overline{(\rho_p)}^{n}_{k+\frac{1}{2}}}, \frac{C_{IO}(\tilde{\alpha}^{n}_{g,\, k+\frac{1}{2}})}{\overline{(\alpha_p\, \rho_p)}^{n}_{k+\frac{1}{2}}}, \left(V^n_p \nabla\, V^n_p\right)_{k+\frac{1}{2}}, ... \Bigg) \tag{2.13}$$

where P is the pressure and $(V_p \nabla\, V_p)^n_{k+\frac{1}{2}}$ the convective phasic velocity terms.

In the aforementioned formulation, quantities like $1/\overline{(\alpha_p\, \rho_p)}^{n}_{k+\frac{1}{2}}$ and $1/\overline{(\rho_p)}^{n}_{k+\frac{1}{2}}$ are cell-length averaged (indicated by a "bar" over them) as follows:

$$\overline{(\alpha_p\, \rho_p)}^{n}_{k+\frac{1}{2}} = \frac{\Delta x_k\, (\alpha_p\, \rho_p)^n_k + \Delta x_{k+1}\, (\alpha_p\, \rho_p)^n_{k+1}}{\Delta x_k + \Delta x_{k+1}} \tag{2.14}$$

where Δx_k, Δx_{k+1} are the cell lengths of the adjacent cells.

As has already been shown elsewhere (Analytis and Coddington, 1992), the numerical modelling of the phasic wall friction $(f_w)_p^n$ in eq.(2.11b) and in particular, the incorporation of the discretized form of this term into the general finite-difference formulation of the phasic momentum equations is of the utmost importance. For our purpose, it is sufficient to note that this term is a function of the square of the total mass flux $G^n_{k+\frac{1}{2}}$ (evaluated at the junction $k+\frac{1}{2}$), i.e.

$$(f_w^n)_{k+\frac{1}{2}} = f\left(\ldots, \left\{\overline{(\alpha_l\,\rho_l)}^{n}_{k+\frac{1}{2}}\; V^n_{l,k+\frac{1}{2}} + \overline{(\alpha_g\,\rho_g)}^{n}_{k+\frac{1}{2}}\; V^n_{g,\,k+\frac{1}{2}}\right\}^2, \ldots\right) \tag{2.15}$$

where all the symbols have their usual meaning, and the terms $\overline{(\alpha_p\,\rho_p)}^{n}_{k+\frac{1}{2}}$ are cell-length averages defined by eq.(2.14).

If we now inspect $(f_w^n)_{k+\frac{1}{2}}$ as given by eq.(2.15) and consider the case in which pure steam $(\alpha_{g,k} = 1)$ from cell k (left) is injected into the cell $(k+1)$ (to the right) containing pure water $(\alpha_{g,k+1} = 0)$. The void fraction $\tilde{\alpha}^{n}_{g,\,k+\frac{1}{2}}$ at the junction $(k+\frac{1}{2})$ between the two volumes is the upwinded void fraction and for our case with $V_{g,\,k+\frac{1}{2}} > 0$, will be equal to 1. Additionally, at this junction one will usually have $|V^n_{l,\,k+\frac{1}{2}}| > 0$ and hence, the wall friction given by eq.(2.15) will attain a high value due to the cell-length averaging of the term $(\alpha_l\,\rho_l)^n_{k+\frac{1}{2}}$ (cf. eq.(2.14)) which will dominate. This leads to an unphysical and high pressure drop between the two adjacent cells. Clearly, for this very simple case, this problem will be most severe when $\alpha_{g,\,k} = 1$ and $\alpha_{g,\,k+1} = 0$ but will always show up when $\alpha_{g,\,k} >> \alpha_{g,\,k+1}$ while for $\alpha_{g,\,k} \sim \alpha_{g,\,k+1}$, it will disappear. For a large multi-component system calculation, one may come across a similar situation on a number of occasions in the course of a transient, but it would be very difficult to quantify.

The most obvious way of eliminating this problem is by modifying the cell-length averaging procedure of the terms $(\alpha_p\,\rho_p)^n_{k+\frac{1}{2}}$ in eq.(2.11a) and employing a donor-cell differencing (upwinding) approach instead. Hence, we now define

$$(\alpha_p\,\rho_p)^n_{k+\frac{1}{2}} = (WP)(\alpha_p\,\rho_p)^n_k + (WP1)(\alpha_p\,\rho_p)^n_{k+1} \tag{2.16}$$

where (WP) and $(WP1)$ are given by eq.(2.12b) and (2.12c). By upwinding these terms (and hence, the total mass flux $G^n_{k+\frac{1}{2}}$), one can see that for our simple steam injection problem, $\tilde{G}^{n}_{k+\frac{1}{2}}$ will be given by (for $V^n_{g,\,k+\frac{1}{2}} > 0$)

$$\tilde{G}^{n}_{k+\frac{1}{2}} = (\alpha_g\,\rho_g)^n_k\; V^n_{g,\,k+\frac{1}{2}} \tag{2.17}$$

There is now no liquid contribution to this term, since $(\alpha_l\,\rho_l)^n_k = 0$ and hence, the wall friction will not attain a very high value. Finally, we should mention that although the origin of the problem was traced to the cell-length averaging procedure used to define the total mass flux in the wall friction terms, we found it "numerically"

advantageous to extend these modifications and upwind all $(\alpha_p\ \rho_p)^n_{k+\frac{1}{2}}$ terms in eqs.(2.11b) and (2.13) as shown in eq.(2.12a). More discussion of this problem is given elsewhere (Analytis and Coddington, 1992). In the present work, we have also included this upwinding option in the discretization of the 3D phasic momentum equations for the vessel in subroutine **TF3E**. We shall further discuss this point in the following section, where we shall present some TLTA calculations; in particular, we shall show that the two different discretization schemes result in different rod surface temperature (RST) histories. Finally, we should mention here that since as we shall discuss later in this section, we found that in general the wall shear model of the code was highly problematic and we decided to change it to the one of TRAC-PF1, it is possible that the reasons for which we had to introduce the upwinding option (Analytis and Coddington, 1992) for some terms of the momentum equations are no longer there. In this work, we did not try to answer this question.

(h) As an option, we introduced the second upwind scheme for the convective terms of the 1D phasic momentum equations (subroutine **TF1E**). When this option is activated, it is only used for the **PIPE** and **CHAN** components. Employment of this scheme for all components resulted in some problems during the analysis of the TLTA test Nr. 6423 whose origin we had no time to investigate. In any case, as we shall discuss in the following section, the employment of this scheme resulted in a little different RST histories for the aforementioned TLTA test when compared to the ones predicted when the donor-cell differencing scheme of TRAC-BF1 is used. The second upwind scheme which is also used in RELAP5, is numerically less diffusive than the one in TRAC-BF1. For any phasic velocity V, we define the quantities

$$\epsilon^- = 0.5|V_{k-\frac{1}{2}} + V_{k+\frac{1}{2}}| \tag{2.18a}$$

and

$$\epsilon^+ = 0.5|V_{k+\frac{1}{2}} + V_{k+\frac{3}{2}}| \tag{2.18b}$$

and the cell-centered velocities

$$V_k = 0.5(V_{k-\frac{1}{2}} + V_{k+\frac{1}{2}}) \tag{2.18c}$$

and

$$V_{k+1} = 0.5(V_{k+\frac{1}{2}} + V_{k+\frac{3}{2}}). \tag{2.18d}$$

Subsequently, we define

$$V_k\tilde{V}_k = V_kV_k + 0.5\epsilon^-(V_{k-\frac{1}{2}} - V_{k+\frac{1}{2}}) \tag{2.19a}$$

and

$$V_{k+1}\tilde{V}_{k+1} = V_{k+1}V_{k+1} + 0.5\epsilon^+(V_{k+\frac{1}{2}} - V_{k+\frac{3}{2}}). \tag{2.19b}$$

An alternative, higher-order accurate scheme which we also implemented (and should be even less diffusive) is one in which ϵ^- and ϵ^+ are defined by:

$$\epsilon^- = 0.5|V_{k-\frac{1}{2}} + V_{k+\frac{1}{2}} - \frac{1}{8}(V_{k+\frac{3}{2}} + V_{k-\frac{1}{2}} - 2V_{k+\frac{1}{2}})| \tag{2.20a}$$

and

$$\epsilon^{+} = 0.5|V_{k+\frac{1}{2}} + V_{k+\frac{3}{2}} - \frac{1}{8}(V_{k+\frac{3}{2}} + V_{k-\frac{1}{2}} - 2V_{k+\frac{1}{2}})| \qquad (2.20b)$$

and subsequently, for the cell-centered velocities

$$V_k = 0.5(V_{k-\frac{1}{2}} + V_{k+\frac{1}{2}} - \frac{1}{8}(V_{k+\frac{3}{2}} + V_{k-\frac{1}{2}} - 2V_{k+\frac{1}{2}})) \qquad (2.20c)$$

and

$$V_{k+1} = 0.5(V_{k+\frac{1}{2}} + V_{k+\frac{3}{2}} - \frac{1}{8}(V_{k+\frac{3}{2}} + V_{k-\frac{1}{2}} - 2V_{k+\frac{1}{2}})), \qquad (2.20d)$$

while finally,

$$\begin{aligned} V_k\tilde{V}_k &= V_kV_k + \\ &0.5\epsilon^{-}(V_{k-\frac{1}{2}} - V_{k+\frac{1}{2}} - \frac{1}{8}(V_{k+\frac{3}{2}} + V_{k-\frac{1}{2}} - 2V_{k+\frac{1}{2}})) \end{aligned} \qquad (2.21a)$$

and

$$\begin{aligned} V_{k+1}\tilde{V}_{k+1} &= V_{k+1}V_{k+1} + \\ &0.5\epsilon^{+}(V_{k+\frac{1}{2}} - V_{k+\frac{3}{2}} - \frac{1}{8}(V_{k+\frac{3}{2}} + V_{k-\frac{1}{2}} - 2V_{k+\frac{1}{2}})). \end{aligned} \qquad (2.21b)$$

Finally, in either case, the convective term can be written as

$$\frac{1}{2}\left(\frac{\partial(V^2)}{\partial z}\right)\Bigg|_k^{k+1} = CONV = \frac{\left(0.5(V_{k+1}\tilde{V}_{k+1} - V_k\tilde{V}_k)\right)}{\Delta x_k^{'}} \qquad (2.22a)$$

where

$$\Delta x_k^{'} = \frac{\Delta x_k + \Delta x_{k+1}}{2} \qquad (2.22b)$$

and Δx_k and Δx_{k+1} are the lengths of the meshes upstream and downstream the junction $k+\frac{1}{2}$. There have been some cases for which a smoother and "less diffusive" behaviour of the code predictions was indeed observed when this scheme was used for the convective terms of the phasic momentum equations. We shall not discuss this issue any further, but we think it is worth investigating.

Before concluding this section, we should say that there are different ways of finite-differencing the spatial part of the virtual mass term in the phasic momentum equations; these we also introduced as an option. The spatial part of the virtual mass term is defined by:

$$f_{vm,g} = k_{vm}\left(\frac{\rho_C(\alpha)}{\alpha\rho_g}\right).V_D\nabla(V_g - V_l) \qquad (2.23a)$$

for the vapour momentum equation and

$$f_{vm,l} = k_{vm}\left(\frac{\rho_C(\alpha)}{(1-\alpha)\rho_l}\right).V_D\nabla(V_l - V_g) \qquad (2.23b)$$

for the liquid, where $V_D = (1-\alpha)V_g + \alpha V_l$, k_{vm} is the virtual mass coefficient and the subscripts C and D are referring to the continuous and dispersed phase, respectively (Taylor et al., 1984, Borowski and Wade, 1992b). In the code, the α in ρ_C at the junction $j+\frac{1}{2}$ is defined by $0.5(\alpha_{j-\frac{1}{2}} + \alpha_{j+\frac{3}{2}})$. Instead, we used the upwinded $\tilde{\alpha}_{j+\frac{1}{2}}$. Furthermore, the finite-differenced term $V_D.\nabla(V_g - V_l)$ is defined in the code as

$$
\begin{aligned}
& V_D.\nabla(V_g - V_l)|_{j+\frac{1}{2}} = \\
& V_{D,j+\frac{1}{2}}\Big((1 + S_{kin})(V_{g,j+\frac{1}{2}} - V_{l,j+\frac{1}{2}} - V_{g,j-\frac{1}{2}} + V_{l,j-\frac{1}{2}}) \\
& +(1 - S_{kin})(V_{g,j+\frac{3}{2}} - V_{l,j+\frac{3}{2}} - V_{g,j+\frac{1}{2}} + V_{l,j+\frac{1}{2}})\Big) \Big/ \Delta x_{j+\frac{1}{2}} \qquad (2.23c)
\end{aligned}
$$

where

$$
S_{kin} = sign(1, V_{D,j+\frac{1}{2}}) \qquad (2.23d)
$$

Instead, we finite-differenced this term as follows:

$$
\begin{aligned}
V_D.\nabla(V_g - V_l)|_{j+\frac{1}{2}} = & \Big(V_{D,j+\frac{1}{2}}\Big[(WV)(V_{g,j+\frac{1}{2}} - V_{g,j-\frac{1}{2}}) + \\
& (1-(WV))(V_{g,j+\frac{3}{2}} - V_{g,j+\frac{1}{2}}) - (WL)(V_{l,j+\frac{1}{2}} - V_{l,j-\frac{1}{2}}) + \\
& (1-(WL))(V_{l,j+\frac{3}{2}} - V_{l,j+\frac{1}{2}})\Big]\Big) \Big/ \Delta x_{j+\frac{1}{2}} \qquad (2.23e)
\end{aligned}
$$

where WL and WV are 1 or 0, depending one whether $V_{l,j+\frac{1}{2}}$ and $V_{g,j+\frac{1}{2}}$ are greater or less than 0, respectively. Notice that with the definition of V_D, during finite-differencing, some of the terms in $V_D.\nabla(V_g - V_l)$ can be expressed by the second upwind formulation discussed in this section.

(i) A simple radiation model similar to the one in RELAP5 was implemented in TRAC-BF1 in the subroutine **HTCOR** holding the heat transfer correlations. The radiation model in the code was found to induce some oscillations and was de-activated from the input in all our runs. Comparison of this very simple model with the sophisticated model in the code revealed very similar temperature histories during the analysis of bottom flooding low flooding rate experiments without the oscillations observed when the original model of the code was used.

(j) As we have already mentioned before, although the employment of the Wallis annular flow interfacial shear correlation (or of the one used in the code but with ρ_l in the place of ρ_g) is necessary if one wants to reproduce results from bottom flooding separate-effect test experiments, this seems to create some problems for some transients. In particular, for the TLTA test Nr. 6423 it leads to a very small time-step approximately 65 seconds after the initiation of the transient. In contrast, the correlation in the code (derived by assuming that in annular flow, the continuous phase is the liquid), always over-predicts the liquid carry-over in bottom flooding tests, but it performs quite reasonably for system calculations. During a number of discussions, it was suggested * that the origin of this problem may lie on the modelling of the wall shear which was also responsible for the pathological

* P. Coddington, Private communication (1996)

behaviour reported elsewhere (Analytis and Coddington, 1992). Hence, in order to investigate this possibility, we implemented in the code the wall shear models of TRAC-PF1 (Liles et al., 1986; Gao and Leslie, 1989), a "heuristic" model which does not "weight" the shear between the wall and the liquid with the liquid fraction, as well as an other simple model similar to the one of TRAC-P in which the wall shear is also separately defined for the two phases. These modifications we implemented in subroutine **FRCW**; though, the 1D phasic momentum equations solution subroutine **TF1E** was also appropriately modified. Before explaining the models, we shall first outline the discretized phasic momentum equations for the 1D components of TRAC-BF1 and the way we had to modify them in order to implement the TRAC-PF1-type wall shear models. The corresponding equations for the vapour and the liquid are written as:

$$\frac{(V_g^{n+1} - V_g^n)_{k+\frac{1}{2}}}{\Delta t} + \underbrace{(V_g^n \delta V_g^n)_{k+\frac{1}{2}}}_{conv.\ term} + \underbrace{\frac{C_{IO}^n (C_1 V_{g,k+\frac{1}{2}}^{n+1} - C_0 V_{l,k+\frac{1}{2}}^{n+1})^q}{\overline{(\alpha\rho_g)}^n_{k+\frac{1}{2}}})}_{(f_i^{n+1}/\overline{(\alpha\rho_g)}^n_{k+\frac{1}{2}}}$$

$$+ \frac{(P_L^{n+1} - P_K^n)}{\overline{\Delta x}_{k+\frac{1}{2}}\ \overline{(\rho_g)}^n_{k+\frac{1}{2}}} + \underbrace{\frac{c_{wg}(V_{g,k+\frac{1}{2}}^{n+1})^2}{\overline{(\alpha\rho_g)}^n_{k+\frac{1}{2}}}}_{f_{wg}^{n+1}/\overline{(\alpha\rho_g)}^n_{k+\frac{1}{2}}} + g\ cos\theta\ = 0 \qquad (2.24a)$$

and

$$\frac{(V_l^{n+1} - V_l^n)_{k+\frac{1}{2}}}{\Delta t} + \underbrace{(V_l^n \delta V_l^n)_{k+\frac{1}{2}}}_{conv.\ term} + \underbrace{\frac{C_{IO}^n (C_1 V_{g,k+\frac{1}{2}}^{n+1} - C_0 V_{l,k+\frac{1}{2}}^{n+1})^q}{\overline{((1-\alpha)\rho_l)}^n_{k+\frac{1}{2}}})}_{(f_i^{n+1}/\overline{((1-\alpha)\rho_l)}^n_{k+\frac{1}{2}}}$$

$$+ \frac{(P_L^{n+1} - P_K^n)}{\overline{\Delta x}_{k+\frac{1}{2}}\ \overline{(\rho_l)}^n_{k+\frac{1}{2}}} + \underbrace{\frac{c_{wl}(V_{l,k+\frac{1}{2}}^{n+1})^2}{\overline{((1-\alpha)\rho_l)}^n_{k+\frac{1}{2}}}}_{f_{wl}^{n+1}/\overline{((1-\alpha)\rho_l)}^n_{k+\frac{1}{2}}} + g\ cos\theta\ = 0 \qquad (2.24b)$$

where overlined quantities indicate that they are cell-length averaged. For the sake of notational convenience, we have ignored the virtual mass terms. As is well-known, in the above equations, the terms with the flow-regime dependent factor C_{IO}^n are due to the interfacial shear (with $q = 2\ or\ 4$ in the different interfacial shear correlations (Taylor et al., 1984), while the ones with the c_{wg} and c_{wl} factors are due to the wall shear. Notice that in the momentum equations (2.24a) and (2.24b), the exponent q is defined by

$$q\ =\ (1 - x_2)q_{bubb}\ +\ x_2((1 - (ent))q_{ann}\ +\ (ent)q_{drp}) \qquad (2.24c)$$

where $q_{bubb} = 4\ (\ = 2\ for\ bundles)$, $q_{ann} = 2$ and $q_{drp} = 4$. $x_2 = 0$ at the void fraction corresponding to the end of the bubbly/slug flow regime and is equal to

1 at the annular-dispersed flow, while (ent) is the entrainment fraction. Hence, in general, the exponent q is not an integer quantity and is defined as above for smoothing purposes.

For each time-step and each junction $k+\frac{1}{2}$, the above system of algebraic equations can be solved as outlined under item (g) above only after **linearising** the interfacial and wall shear terms so that the new-time phasic velocities appear linearly. We do this by approximating (Taylor et al., 1984)

$$f_i^{n+1} \simeq C_I^n \Big(-(q-1)\,(V_R^n)^q + q(V_R^n)^{q-1}\,(V_R^{n+1}) \Big). \tag{2.25a}$$

for the interfacial shear term (where $V_R = (C_1 V_g - C_0 V_l)$), and

$$f_{wl}^{n+1} \simeq c_{wl} \Big(-(V_l^n)^2 + 2(V_l^n)\,(V_l^{n+1}) \Big), \tag{2.25b}$$

$$f_{wg}^{n+1} \simeq c_{wg} \Big(-(V_g^n)^2 + 2(V_g^n)\,(V_g^{n+1}) \Big). \tag{2.25c}$$

for the wall shear. Though, the aforementioned linearization of the wall shear terms is not used in TRAC-BF1. The general modelling of the wall shear in the code is done as follows: We first define

$$c_{fl} = \frac{\left|\frac{dp}{dz}\right|_{wf}^{n}}{\rho_l^n (V_l^n)^2} \tag{2.26a}$$

and

$$c_{fg} = \frac{\left|\frac{dp}{dz}\right|_{wf}^{n}}{\rho_g^n (V_g^n)^2} \tag{2.26b}$$

where the subscript wf means "wall friction". At the end-of-time step, the total pressure gradient due to the wall friction is divided between the phases using the void fraction as a measure of the surface area in the cell "melted" by each phase; we obtain

$$\left|\frac{dp}{dz}\right|_{wf,g}^{n+1} = \alpha \left|\frac{dp}{dz}\right|_{wf}^{n+1} = (\alpha^n)^2 \rho_g^n c_{fg} V_g^n V_g^{n+1} + \alpha^n (1-\alpha^n) \rho_l^n c_{fl} V_l^n V_l^{n+1} \tag{2.26c}$$

and

$$\left|\frac{dp}{dz}\right|_{wf,l}^{n+1} = (1-\alpha) \left|\frac{dp}{dz}\right|_{wf}^{n+1} = (\alpha^n)(1-\alpha^n) \rho_g^n c_{fg} V_g^n V_g^{n+1} + (1-\alpha^n)^2 \rho_l^n c_{fl} V_l^n V_l^{n+1} \tag{2.26d}$$

In principle, one could easily linearise the above wall shear model along the lines of eqs (2.25b) and (2.25c) by approximating the implicit phasic velocity products $V^{n+1}V^{n+1}$ by $(2V^nV^{n+1} - (V^n)^2)$ rather than by $V^{n+1}V^{n+1}$ as done in eqs. (2.26c) and (2.26d). As we said before, these terms are not linearised in the code, although we have included such a linearization as an option if the original wall shear model of the code is used. Due to the special form of this model, both the liquid and vapour wall shear contributions are appearing in each of the phasic momentum equations (Borowski and Wade, 1992b); in particular, the former is the wall shear entering the vapour and the latter, the liquid momentum equations, respectively. In assessing the different wall shear models, we also corrected a logic error in the subroutine **TF1E** solving the phasic momentum equations, in which the calculated wall shear coefficients were not re-set to 0 if there were back-ups. *

In order to investigate the possible relation of the aforementioned problems with the wall shear model in the code, we implemented in TRAC-BF1 the wall shear models of TRAC-PF1 (Liles et al., 1986; Gao and Leslie, 1989). In these models, the wall shear of the liquid appears in the liquid momentum equation and the one of the vapour in the vapour momentum equation. The TRAC-PF1 models are the **homogeneous** and **annular flow** models and can be summarised as follows:

I. Homogeneous Model

The pressure drop due to the wall friction is generally calculated from

$$\left|\frac{dp}{dz}\right|_{wf} = c_{wg}V_g^2 + c_{wl}V_l^2 \tag{2.27}$$

where c_{wg} and c_{wl} are defined by

$$c_{wg} = \frac{\alpha\rho_g c_{fg}}{D_H} \tag{2.28a}$$

and

$$c_{wl} = \frac{(1-\alpha)\rho_l c_{fl}}{D_H} \tag{2.28b}$$

Then, the frictional pressure drop can be written as

$$\left|\frac{dp}{dz}\right|_{wf} = \frac{\alpha\rho_g c_{fg}V_g^2}{D_H} + \frac{(1-\alpha)\rho_l c_{fl}V_l^2}{D_H} \tag{2.29}$$

In the homogeneous model, the friction coefficients c_{fg} and c_{fl} are calculated as follows:

$$c_{fl,hom} = 2f \tag{2.30}$$

$$\begin{aligned} c_{fg,hom} &= 2f, && if\ \alpha \le 0.9 \\ &= (10\alpha - 9)^2(21 - 20\alpha)c_{fl,hom}, && if\ \alpha > 0.9 \end{aligned} \tag{2.31}$$

* P. Coddington, Private communication (1996)

Finally, f is defined by

$$\begin{aligned} f &= 0.032, && if\ Re \leq 500 \\ &= 0.032 - 5.25\,10^{-6}(Re - 500), && if\ 500 < Re < 5000 \\ &= 0.046(Re)^{-0.2}, && if\ Re > 5000. \end{aligned} \tag{2.32a}$$

where

$$Re = \frac{GD_H}{\mu_m}, \qquad G = \rho_m V_m. \tag{2.32b}$$

The mixture viscosity μ_m is calculated by

$$\frac{1}{\mu_m} = \frac{x}{\mu_g} + \frac{1-x}{\mu_l} \tag{2.32c}$$

and the flow quality x by

$$x = \frac{1}{1 + \dfrac{(1-\alpha)\rho_l V_l}{\alpha \rho_g V_g}} \tag{2.32d}$$

Finally, the mixture density and velocity are defined by

$$\rho_m = \alpha\rho_g + (1-\alpha)\rho_l \tag{2.32e}$$

and

$$V_m = \alpha\rho_g V_g + (1-\alpha)\rho_l V_l \tag{2.32f}$$

II. Annular Flow Model

By this, it is not actually implied that flow is annular, but it is just a "label" given to this particular model. In this model, the wall friction coefficients are given by

$$\begin{aligned} c_{fl} &= 2f, && if\ \alpha \leq 0.9 \\ &= (1-w_f)2f + w_f c_{fl,hom}, && if\ 0.9 < \alpha \leq 0.9995 \\ &= c_{fl,homo}, && if\ \alpha > 0.9995 \end{aligned} \tag{2.33a}$$

and

$$\begin{aligned} c_{fg} &= 0, && if\ \alpha \leq 0.9 \\ &= (10\alpha - 9)^2(21 - 20\alpha)c_{fl}, && if\ 0.9 < \alpha \leq 0.9995 \\ &= c_{fg,homo}, && if\ \alpha > 0.9995 \end{aligned} \tag{2.33b}$$

where

$$w_f = \frac{(\alpha - 0.9)}{0.0995} \tag{2.33c}$$

Then, the friction factor f is defined as

$$f = f_{sp}\phi^2 \tag{2.34a}$$

where

$$f_{sp} = a + \frac{b}{(Re)^c} \tag{2.34b}$$

with

$$a = 0.026\left(\frac{k}{D_H}\right)^{0.225} + 0.133\left(\frac{k}{D_H}\right) \tag{2.34c}$$

$$b = 22\left(\frac{k}{D_H}\right)^{0.44} \tag{2.34d}$$

$$c = 1.62\left(\frac{k}{D_H}\right)^{0.134} \tag{2.34e}$$

where $k = 5\ 10^{-6}$, while the Reynolds number is the same like the homogeneous model. Finally, ϕ^2 is given by

$$\phi^2 = \frac{\rho_l}{\rho_m}. \tag{2.34f}$$

In implementing the aforementioned TRAC-PF1 wall shear models in the code, we also linearised the wall shear term (cf. eq. (2.25b), (2.25c))

III. No Weighting of Wall-Friction to the Liquid

Although even in the TRAC-PF1 model the wall shear is "weighted" with the corresponding phasic fraction, in reality, this is not the case and eg in annular flow, the wall shear force acts only on the liquid film and not on the vapour or the droplets. For this, in addition to the TRAC-PF1 models, we implemented in the code a logic according to which eq. (2.31) reads

$$\begin{aligned} c_{fg} &= 2f, && if\ \alpha \leq 0.96 \\ &= (10\alpha - 9.6)^2(21 - 20\alpha)c_{fl}, && if\ \alpha > 0.96 \end{aligned} \tag{2.35}$$

while eq. (2.29) is modified as

$$\left|\frac{dp}{dz}\right|_{wf} = \frac{\alpha\rho_g c_{fg} V_g^2}{D_H} + \frac{(WAWET)\,\rho_l c_{fl} V_l^2}{D_H}, \tag{2.36}$$

where $WAWET$ is internally defined in the code and represents the fraction of the particular volume which is in contact with the liquid: $WAWET = 1$ indicates that the wall of the volume is wet, while $WAWET = 0$ indicates that it is dry. The aforementioned logic does actually somehow captures the fact that if the wall is wet, the wall shear is only between the wall and the liquid and is not actually "weighted" with the liquid fraction. In implementing all the three aforementioned wall shear models in the code, we also linearised the wall shear term (cf. eq. (2.25b), (2.25c)).

Concluding, we should say that in addition to the models above, we have recently tried and implemented in the code two more wall friction models with equally successful results. In the first model, c_{fl} and c_{fg} in eqs. (2.28a) -(2.28b) are given by

$$c_{fl} = \lambda_l f(Re_l), \tag{2.37a}$$

$$c_{fg} = \lambda_g f(Re_g), \tag{2.37b}$$

where Re_p denotes the Reynold's number of the phase p; eg for the vapour,

$$Re_g = \frac{\alpha \rho_g V_g D_H}{\mu_g}. \tag{2.37c}$$

The ramp function λ is defined by

$$\begin{aligned} \lambda_g &= 0, && if\ \alpha < 0.999 \\ &= \frac{\alpha - 0.999}{0.0009}, && if\ 0.999 \leq \alpha \leq 0.9999 \\ &= 1, && if\ \alpha > 0.999 \end{aligned} \tag{2.37d}$$

$$\lambda_l = 1 - \lambda_g. \tag{2.37e}$$

The friction factor $f(Re_p)$ is for smooth pipes and is defined by

$$f(Re_p) = \frac{1}{2}\, max\left(\frac{64}{Re_p}, 0.0055 + \frac{0.55}{(Re_p)^{0.333}}\right) \tag{2.37f}$$

while for turbulent flow ($Re_p > 5000$), we use

$$f(Re_p) = \frac{1}{2}\left(\frac{0.046}{Re_p^{0.2}},\right) \tag{2.37g}$$

In the second model which is the Churchill's model, * one first defines

$$ff = \left(\left(\frac{8.0}{Re}\right)^{12.0} + \frac{1}{(aa + bb)^{1.5}}\right)^{cc} \tag{2.38a}$$

where aa, bb and cc are defined by

* D.R. Page, Penn State University, Private communication (1997)

$$aa = \left(2.457 \, log \left(\frac{1}{\left(\frac{7}{Re} \right)^{0.9} + 0.27\epsilon_d} \right) \right)^{16}, \tag{2.38b}$$

$$bb = \left(\frac{37530}{Re} \right)^{16}, \tag{2.38c}$$

$$cc = \frac{1}{12}, \tag{2.38d}$$

where ϵ_d is the surface roughness divided by the hydraulic radius (half the hydraulic diameter) and the Reynold's number Re is defined by eq. (2.32b). Then, c_{fl} and c_{fg} in eqs. (2.28a) -(2.28b) are given by

$$c_{fl} = 4 \, ff, \tag{2.39a}$$

$$c_{fg} = c_{fl}, \tag{2.39b}$$

A number of runs of different problems was also made with the aforementioned wall shear models; in all cases, the results were rather similar to the ones obtained when the TRAC-PF1 homogeneous wall shear model was activated; hence, in this work, we shall not report on these results.

3 ASSESSMENT OF THE MODIFIED CODE AND COMPARISON WITH THE FROZEN VERSION

3.1 The NEPTUN bottom flooding tests

In this section, we shall analyse 3 bottom flooding tests in the NEPTUN test facility at PSI. Some of the important boundary conditions of the tests are summarised below:

Nr. 5036 (P = 4.1 bar, ΔT_s = 10 K, V_{IN} = 0.015 m/s),

Nr. 5050 (P = 4.1 bar, ΔT_s = 78 K, V_{IN} = 0.15 m/s),

Nr. 5052 (P = 4.1 bar, ΔT_s = 78 K, V_{IN} = 0.025 m/s),

In the analysis of the bottom flooding experiments presented here with the modified version of TRAC-BF1, we have used for annular flow the interfacial shear correlation in the code but with ρ_g in place of ρ_l (i.e. equivalent to the original Wallis correlation; see

Section 2 under (g)). Additionally, we have made all the runs by using the upwinding option described in section 2 under (e). In a previous work (Analytis and Coddington, 1992), we have shown that for these experiments, the differences between the predictions obtained by using the upwinding and the standard code cell-length average approach are almost non-observable. Furthermore, we shall present some results obtained with the modified version of the code but with the Bharathan annular flow interfacial shear correlation of RELAP5/MOD2 and compare them with the results obtained by using the Wallis correlation.

In Fig.1 - 8, we compare for these 3 tests the collapsed liquid level (CLL), RST histories and HTCs to the liquid and void fractions obtained by the frozen and modified versions of the code with the corresponding measurements. Clearly, for all 3 experiments, the predictions of our modified version are very close to the measurements. In particular, for test Nr. 5036, the large differences between the measured and predicted RSTs are not only due to modelling of the wall-to-liquid HTC during reflooding, but also due to the excessively high liquid carry-over predicted by the frozen version of the code, as a result of the high annular flow interfacial shear, a problem we already discussed in the previous section (the runs with the modified code were made with the annular flow interfacial shear in which the continuous phase is assumed to be the vapour eg, we have used ρ_g instead of ρ_l). All the NEPTUN runs were made with the original wall shear model of the code; analysis of one case with the TRAC-PF1 wall shear models discussed in this work (and the upwinding option switched-off) did not show any significant differences and the very good agreement between measurements and predictions prevailed. Hence, we do not show these runs here.

In Fig.9 - 12, we show the same comparisons for the NEPTUN tests Nr. 5036 and 5052, but with the Bharathan annular flow interfacial shear correlation activated. If we compare these predictions with the corresponding ones shown before, one can clearly see that for the tests in which the code does assume annular flow for some time during the transient, the CLLs are now lower than before. This indicates that the Bharathan annular flow interfacial shear is higher than the one of Wallis, but still lower than the one used in the frozen version of the code. Consequently, the different elevations quench later than before, since now there is less liquid in the bundle.

3.2 A top flooding benchmark test

In this section, by using the input deck of the NEPTUN exp. Nr. 5036, we shall simulate a top flooding benchmark test with the same initial and boundary conditions as the ones of the real, bottom flooding test. The aim of this is to assess the way the code performs under "clean" top flooding conditions. In doing this, we shall point out all the problems arising from the modelling of the annular flow interfacial shear as well as the effect of the wall shear model on the code predictions. The CCFL flag was activated at the top node of the test-section.

In our analysis, we shall compare different predicted variables of interest by analysing the case with 3 different code versions: The modified one with the Wallis annular flow

interfacial shear correlation and the TRAC-PF1 "annular flow" wall shear option, the modified one with Wallis correlation and the wall shear model of the frozen version, and finally the frozen version of the code. In Fig.13, we compare the predicted CLLs, in Fig.14 the RSTs at 6 different axial elevations and in Fig.15, the predicted liquid velocities, also at 6 different axial elevations. By inspecting these figures, one can readily draw the following important conclusions:

(a) Similarly to the bottom flooding tests, the frozen version of the code excites oscillations which result in spontaneous CLL depletions. The result of this is that the RSTs are reaching very high values due to liquid deficiency in the test section and the fact that before the liquid reaches the bottom of the rod bundle and starts accumulating, is being sporadically expelled. Similarly to the corresponding **real** bottom flooding test, the elevations in the middle of the rods do not quench. There are various reasons for this behaviour, one of them being the wrong modelling of the HTC during reflooding as discussed in this work.

(b) With the frozen version, the liquid velocities are exhibiting large-amplitude spikes resulting in excessive liquid carry-over from the test-section. In the upper parts of the core, there exists a small negative liquid velocity (indicating a kind of falling film) which is suddenly interrupted spontaneously (and reverses sign) by the aforementioned large liquid velocity spikes. The creation of the "film" at the higher elevations is due to the very high annular flow interfacial shear used in the frozen version of the code as we discussed in this work, which results in creating and holding-up the film at the top of the rods.

(c) When the modified code is used with the Wallis annular flow interfacial shear correlation but with the standard wall friction package, the liquid velocities are now everywhere large and negative and there is hardly any film formed at the top of the rods due to the low annular flow interfacial shear which pushes the liquid to the bottom of the test-section. Clearly, the wall shear is too low to hold the liquid film. We have already discussed this problem in this work.

(d) When the modified code with the Wallis annular flow interfacial shear correlation but also with the wall shear correlation of TRAC-PF1 is used, the predictions look much more reasonable and physically sound. In particular, there is a slowly downwards-progressing film from the top of the rods and all predicted quantities are free of unphysical oscillations. In particular, the liquid velocities are well-behaved and free of spurious and unphysical oscillations.

3.3 The TLTA Test 6423

The description of the TLTA facility and tests are described elsewhere (Taylor et al., 1984), while the input deck used for the analysis reported in this work was the one which was used by the code developers and was sent to us together with the code. In this work, we shall report on the analysis of the TLTA test Nr. 6423. The same test was analysed in the past (Analytis, 1992; Analytis and Coddington, 1992); though, since our final code

version is now a little different to the one we used in the previous work, we shall repeat here the calculations by using different options, and compare the predictions with the ones of the frozen version of the code as well as with the measurements. The results of our comparisons in the past showed that for this particular test, the predicted RST histories are sensitive to the discretization scheme used in the solution of the 1D and 3D phasic momentum equations (i.e., to whether some of the terms are upwinded or not).

In Fig.16, we show the maximum RST history predicted by the frozen version of the code **with the fine-mesh switched-on**, and we compare it to the measured one. Clearly, as also shown and discussed in the past (Analytis, 1992), the predicted RST history is not agreeing with the measurements: The peak RST is approximately 320 K higher than the measured one and quenching occurs much later (approximately up to over 350 s later than the measurements show). Furthermore, the axial elevation exhibiting the peak RST is different (lower) than the corresponding ones when the test is analysed with our modified versions. It is worth reminding the reader that as has already been pointed out (Analytis, 1992), in contrast to these predictions, if the upwinding scheme described under (g) above is used, even with the frozen version of the code the differences between measurements and predictions are no longer so large. We shall not discuss this point any further since as we have already extensively elaborated in this work, independently of whether the predictions of the frozen version for this test are much better if this scheme is used, there are a number of problems with some of the physical models in the code.

In Fig.17, we compare the measured and predicted maximum RST history for the TLTA test Nr. 6423 by using the modified version of the code, both with the standard and upwinding options in the 1D phasic momentum equations. The CCFL modifications of the distribution coefficients C_0 and C_1 in the interfacial shear subroutines are activated (as explained in the previous section) only if the CCFL model is activated for that junction. One can see that although the modified code over-predicts the maximum RST by 50 K when the upwinding option is used, the predicted RST(s) are close to the measured one. Notice that the modified code does not predict the first dry-out.

The upwinding used in the case shown in Fig.17 was only for the 1D components. In Fig.18, we show a comparison of the predicted maximum RST history for the same TLTA test by using the modified version in which the upwinding option is activated both for the 1D and 3D components, with the one in which the upwinding option is used only in the 1D components (as in Fig.17). Clearly, although the peak RST is for both cases almost the same, when the upwinding option is used in all components, quenching occurs later, following a plateau-type region of the RST. In other axial elevations (not shown here), the peak RST of the nodes as well as the dry-out times are also a little different.

Finally, in Fig.19, we compare the predictions of the modified code with the Wallis annular flow interfacial shear correlation (i.e. by setting ρ_g in the place of ρ_l in the Andersen annular flow interfacial shear correlation in subroutine FRCIF), but with three different wall shear models: The homogeneous and annular flow model ones of TRAC-PF1 and a rather "heuristic" one in which the shear between the wall and the liquid is not "weighted" with the liquid fraction, but rather with the fraction of the volume which is wet. The upwinding option was not activated in these runs. One can clearly see that all the runs are completed without any problems. In contrast, with the original wall shear

model and the Wallis annular flow interfacial shear, it is very difficult to run this case due to the fact that as we said before, after 65 s, the code was selecting very small time-steps.

Concluding this section we should mention that we have also analysed this test by activating the second upwind scheme in the phasic momentum equations (for the CHAN and PIPE components; see previous section under (h)). The predictions by analysing the test with this option were very close to the ones obtained by using the standard scheme in the code and in actual fact, exhibited some characteristics indicating less numerical diffusion as compared to the results obtained by using the standard model in the code. In any case, the main message conveyed from the analysis of this test by the frozen and modified versions of the code is that as it is patently clear from Fig.16, the frozen version, for a number of reasons, cannot even remotely predict the peak RST history.

4 CONCLUDING DISCUSSIONS

In this work, we reported on a series of model changes and options implemented in TRAC-BF1. Some of these changes are a little different to the ones reported in a previous work (Analytis, 1992) while some of the implemented options are new and serve to assess not only physical models, but are also related to numerics. The main conclusions of our work can be summarised as follows:

(a) The implemented empirical wall-to-liquid HTC activated in the code during reflooding seems to perform very well. In particular, analysis of a number of NEPTUN bottom flooding experiments with the new version of the code showed very good agreement between measurements and predictions. Though, to achieve this good agreement, one had to use the Wallis annular flow interfacial shear correlation which assumes that the continuous phase is the vapour, instead of the one already in the code which although based on the same correlation, is derived by assuming that the continuous phase is the liquid, which results in a factor ρ_l as a multiplier. This makes the shear excessively high and in the case of bottom flooding, can greatly deplete the liquid inventory.

(b) Two different annular flow interfacial shear correlations were implemented and tested in the code and in addition to the Wallis correlation (being the same one like the one already in the code but with ρ_g instead of ρ_l) which seems to give good predictions for bottom flooding experiments (in which this flow regime is activated in the code), we also implemented as an option the Bharathan annular flow interfacial shear correlation as used in RELAP5/MOD2. Clearly, due to the particular simple flow-regime map of TRAC-BF1 (bubbly/slug flow on the one end, annular/mist on the other and interpolation between), if during a particular transient the annular/mist flow interfacial shear is activated (which is the case, if the wall is wet and the liquid fraction is rather small), the code predictions are bound to be very sensitive to the actual functional form of that particular interfacial shear correlation. We have shown that within the framework of the TRAC-BF1 flow-regime map, for bottom flooding, while the Wallis annular flow interfacial shear correlation tends to be a little too low

resulting in a small over-prediction of the liquid inventory, the one of Bharathan exhibits the opposite effect, both of them being in general quite acceptable.

(c) The new approach for letting the liquid velocity approach the one of the vapour as the liquid disappears seems to work well and is superior to the one we used in a previous work (Analytis, 1992).

(d) We have shown that the RST histories obtained for the TLTA test Nr. 6423 are very close to the measured ones whether the standard cell-length averaging or upwinding schemes are used for some terms of the phasic momentum equations. Also a number of calculations for this test were performed with the modified code **including the new wall shear package of TRAC-PF1**, and the same good agreement between measurements and predictions resulted. The second upwind scheme used in the finite-differencing of the convective terms of the 1D phasic momentum equations was also tested (only if the component was a CHAN or a PIPE) and the code predictions were also very close to the ones obtained when the first upwind scheme is used. The second upwind scheme should be numerically less diffusive than the one used in the code. Furthermore, we have shown that for this test, the RST histories predicted by the unmodified code are not even remotely near the measurements, indicating the inevitable general inability of the frozen version of the code to model reflooding, but also a number of other problems from which the frozen version is plagued.

(e) A number of outstanding problems related to the modelling of the annular flow interfacial shear were investigated by changing the wall shear model of the code and implementing the one of TRAC-PF1. By doing this, the Wallis annular flow interfacial shear correlation could be used independently of whether we were modelling separate-effect bottom flooding tests, top flooding tests or "system" calculations like the TLTA. In particular, a number of problems which under certain conditions manifested themselves when the Wallis annular flow interfacial shear correlation was activated in the code were actually due to the wall shear model; most of these problems were eliminated when the wall shear model was changed. A top-flooding benchmark test was also analysed with different versions of the code (including the frozen version) and the problems with the wall shear model of the code were clearly identified. In view of all these we would strongly recommend changing the wall shear model in the code which seems to create a number of problems in favour of an alternative one.

Concluding, we should say that although at least as far as physical models are concerned, this work is restricted to a rather limited area in the code (wall heat transfer during reflooding and interfacial and wall shear), there are certainly a number of other problems which require attention as well as models whose improvement would be highly desirable. Our general recommendations in relation to the problems analysed and discussed in this work can be summarised as follows:

(a) **Implementation of a wall-to-liquid HTC during reflooding which takes into account the distance from the upper or lower QFs. Such a correlation was**

successfully used in this work and its physical and realistic behaviour clearly demonstrated. This model is already implemented in the code by the Penn State University team and delivered to the US Nuclear Regulatory Commission (NRC).

(b) During reflooding, since the CHF is only used indirectly and we are not actually interested in the exact value of this quantity, it would be beneficial to use a simple CHF correlation similar to the one used in this work, which exhibits a smooth behaviour. This will greatly damp oscillations excited during reflooding whose origin can sometimes be traced back to the complex functional form of the CHF used in the transition boiling.

(c) Implementation of the high void fraction single-phase limit in the momentum equations as explained in this work.

(d) Modification of the C_0 and C_1 coefficients in the interfacial shear subroutine FRCIF ONLY IF there is really CCFL.

(e) Implementation of the right annular flow interfacial shear in the code by changing the liquid density in the correlation to the vapour density (Wallis correlation as in TRAC-PF1 and RELAP5/MOD3).

(f) Changing the wall friction model of the code which seems to induce a number of problems in favour of a model similar to the one in TRAC-PF which does not express the wall friction in terms of total pressure drop (and hence, subsequently requiring partitioning of the shear between the two phases), but separately as wall friction on the vapour and the liquid. Ideally, one would need a model which eg in annular flow, would account for the fact that the wall friction is ONLY between the wall and the liquid. This modification may also render the upwinding scheme of some terms of the phasic momentum equations reported in this work unnecessary. Both items (e) and (f) will be parts of the new version of the code.

(g) A further investigation of the advantages of using a second-upwind type scheme for the convective terms of the phasic momentum equations is worth pursuing. Furthermore, the possible extension of the code for accommodating an additional liquid field would be desirable.

Acknowledgements

We would like to thank Paul Coddington with whom we had a number of discussions in the past. In particular, the investigation of the effect of upwinding some terms of the phasic momentum equations was performed jointly with him, while a number of recent discussions led to the study of the shortcomings of the wall shear model in the code.

References

G. TH. ANALYTIS, *Trans. Amer. Nucl. Society*, **52**, 481 (1986).

G. TH. ANALYTIS, Developmental Assessment of TRAC-BF1 with Separate-Effect and Integral Reflooding Experiments. NURETH-5 Conference, 21-24/9/1992, Salt Lake City, Utah, U.S.A., Vol. I, pp 287 - 293 (1992).

G. TH. ANALYTIS, *Trans. Amer. Nucl. Soc.*, **73**, 512 (1995).

G. TH. ANALYTIS, Development and assessment of a modified version of RELAP5/MOD3, NURETH-7 Conference, 10- 15/9/1995, Troy, New York (1995).

G. TH. ANALYTIS, Developmental Assessment of RELAP5/MOD3.1 with Separate-Effect and Integral Test Experiments: Model Changes and Options, PSI Report Nr. 96-09 (April 1996); *Nucl. Engng and Dsgn*, Vol. 163, 125 (1996).

G. TH. ANALYTIS and P. CODDINGTON, The effect of donor cell differencing of some terms of the momentum equations of TRAC-BF1 on code predictions, NURETH-5 Conference, 21- 24/9/1992, Salt Lake City, Utah, U.S.A., Vol. II, pp 287 - 293 (1992).

J.G.M ANDERSEN, K.H. CHU AND J.C. SHAUG, BWR Refill-Reflood Program Task 4.7 - Model Development: Basic Models for the BWR Version of TRAC, NUREG/CR-2573 (1983).

D. BESTION, Interfacial Friction Determination for the 1D-6-Equations Two-Fluid Model used in the CATHARE Code. Paper presented at the European Two-Phase Flow Group Meeting, Southampton, U.K., June 3-7, 1985.

D. BESTION, The Physical Closure Laws in the CATHARE code, *nucl. Engng and Dsgn*, 124, pp 229 - 245 (1990).

J. A. BOROWSKI AND N. L. WADE (Editors), TRAC-BF1/MOD1: An Advanced Best-Estimate computer Program for BWR Accident Analysis: Model Description, NUREG/CR-4356, EGG-2626, Vol. 1 (1992a).

J. A. BOROWSKI AND N. L. WADE (Editors), TRAC-BF1/MOD1 Models and Correlations, NUREG/CR-4391, EGG-2680, (1992b).

K. E. CARLSON et. al., RELAP5/MOD3 Code Manual Volume IV: Models and correlations (Draft), June 1990.

S. GAO and D. C. LESLIE, Two-fluid Modeling of Vertical Annular Two-Phase Flow, Report AERE-R13633, AERE Harwell (1989).

H. GRÜTER, F. STIERLI, S. N. AKSAN and G. VARADI, NEPTUN Bundle reflooding experiments: Test Facility description: EIR Report Nr. 386 (1980).

M. ISHII, One-Dimensional Drift-Flux Model and Constitutive equations for Relative Motion Between Phases in Various Two-Phase Flow Regimes, ANL-77-47 (1977).

D. JUHEL, A Study on Interfacial and Wall Heat Transfer downstream a Quench Front, in "The First International Workshop on Fundamental Aspects of Post-Dryout Heat Transfer," NUREG/CP-0060, pp 179-203 (1984).

D. R. LILES et. al., TRAC-PF1/MOD1: An Advanced Best-Estimate computer Program for Pressurized Water Reactor Thermal-Hydraulic Analysis NUREG/CR-3858, LA-10157-MS, 1986.

V. H. RANSOM et. al., RELAP5/MOD2 Code Manual Volume 1: Code Structure, System Models and Solution Methods, NUREG/CR-4312, (1985).

L. D. TAYLOR et. al., TRAC-BD1: An Advanced Best-Estimate Computer Program for Boiling Water Reactor Transient Analysis, NUREG/CR-3633 (1984).

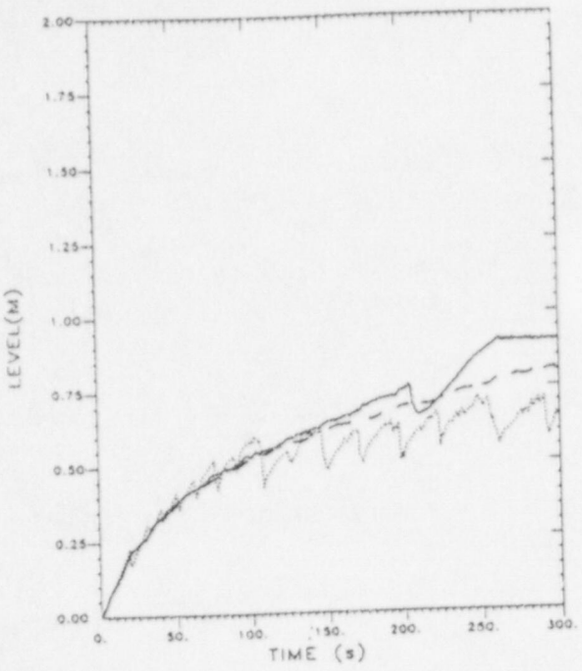

Fig.1 NEPTUN bottom flooding exp. Nr. 5036. Collapsed Liquid Level (m) . (——): Modified TRAC-BF1; (.....): frozen version; (- - -): measurements.

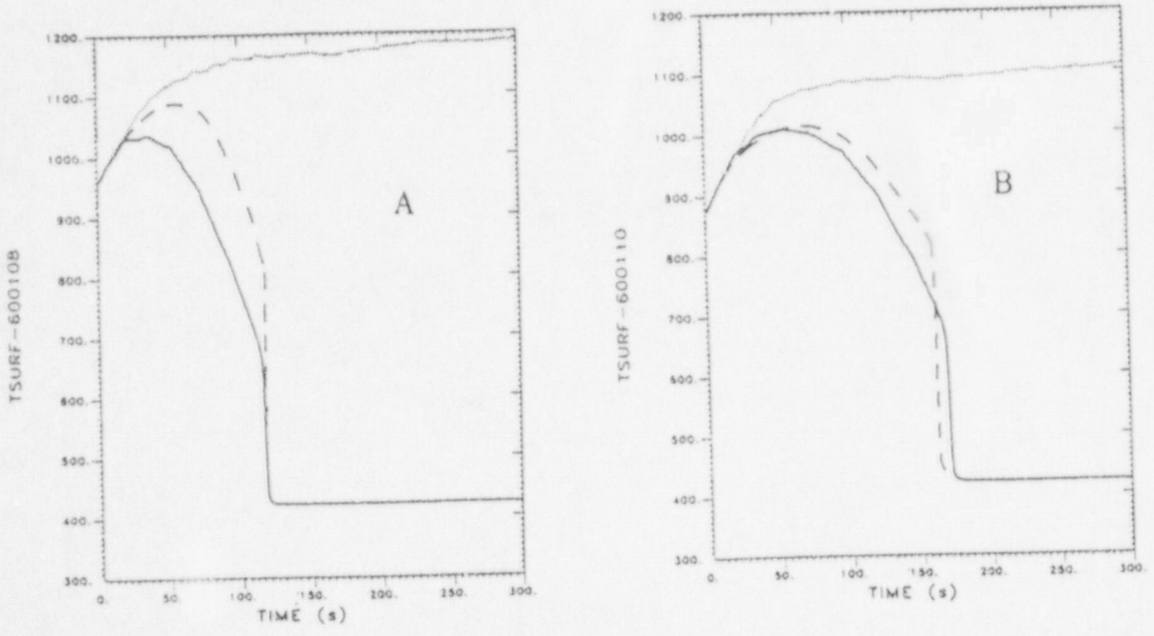

Fig.2 NEPTUN bottom flooding exp. Nr. 5036. RSTs (K) at axial elevations 0.714 m (A) and 0.946 m (B). (——): Modified TRAC-BF1; (.....): frozen version; (- - -): measurements.

M. ISHII, One-Dimensional Drift-Flux Model and Constitutive equations for Relative Motion Between Phases in Various Two-Phase Flow Regimes, ANL-77-47 (1977).

D. JUHEL, A Study on Interfacial and Wall Heat Transfer downstream a Quench Front, in "The First International Workshop on Fundamental Aspects of Post-Dryout Heat Transfer," NUREG/CP-0060, pp 179-203 (1984).

D. R. LILES et. al., TRAC-PF1/MOD1: An Advanced Best-Estimate computer Program for Pressurized Water Reactor Thermal-Hydraulic Analysis NUREG/CR-3858, LA-10157-MS, 1986.

V. H. RANSOM et. al., RELAP5/MOD2 Code Manual Volume 1: Code Structure, System Models and Solution Methods, NUREG/CR-4312, (1985).

D. D. TAYLOR et. al., TRAC-BD1: An Advanced Best-Estimate Computer Program for Boiling Water Reactor Transient Analysis, NUREG/CR-3633 (1984).

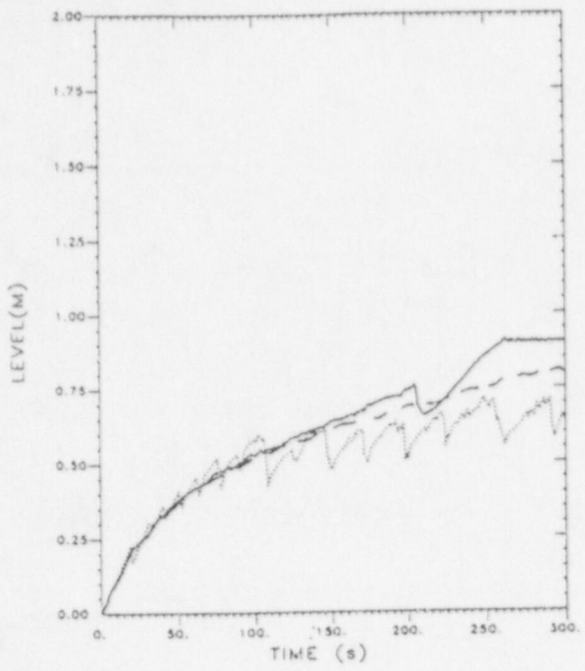

Fig.1 NEPTUN bottom flooding exp. Nr. 5036. Collapsed Liquid Level (m) . (——): Modified TRAC-BF1; (.....): frozen version; (- - -): measurements.

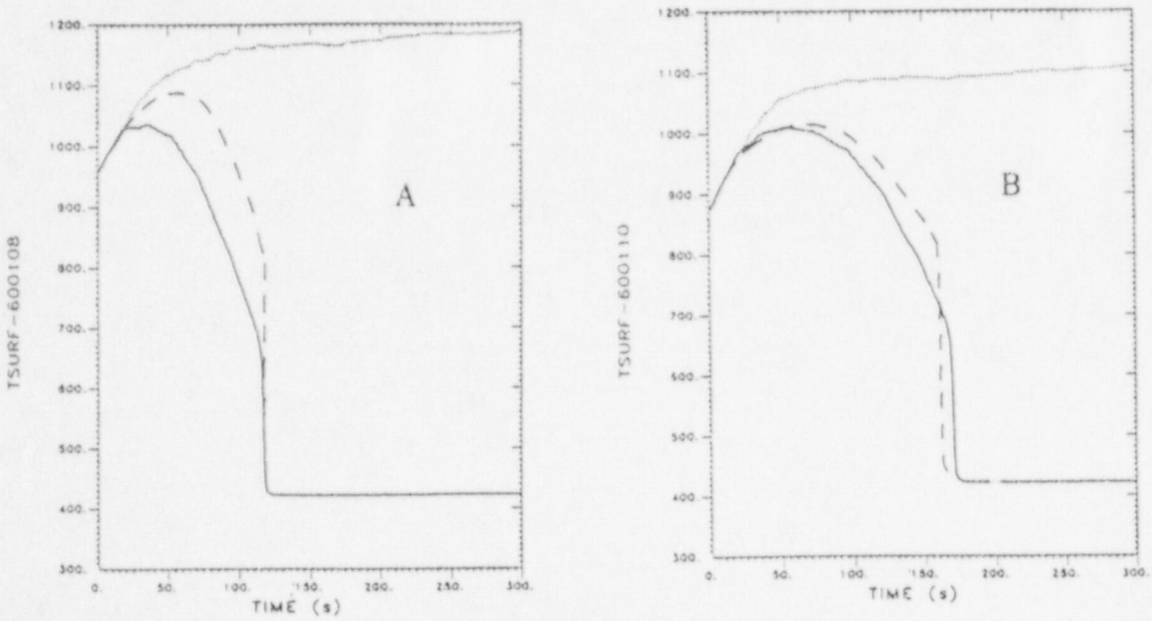

Fig.2 NEPTUN bottom flooding exp. Nr. 5036. RSTs (K) at axial elevations 0.714 m (A) and 0.946 m (B). (——): Modified TRAC-BF1; (.....): frozen version; (- - -): measurements.

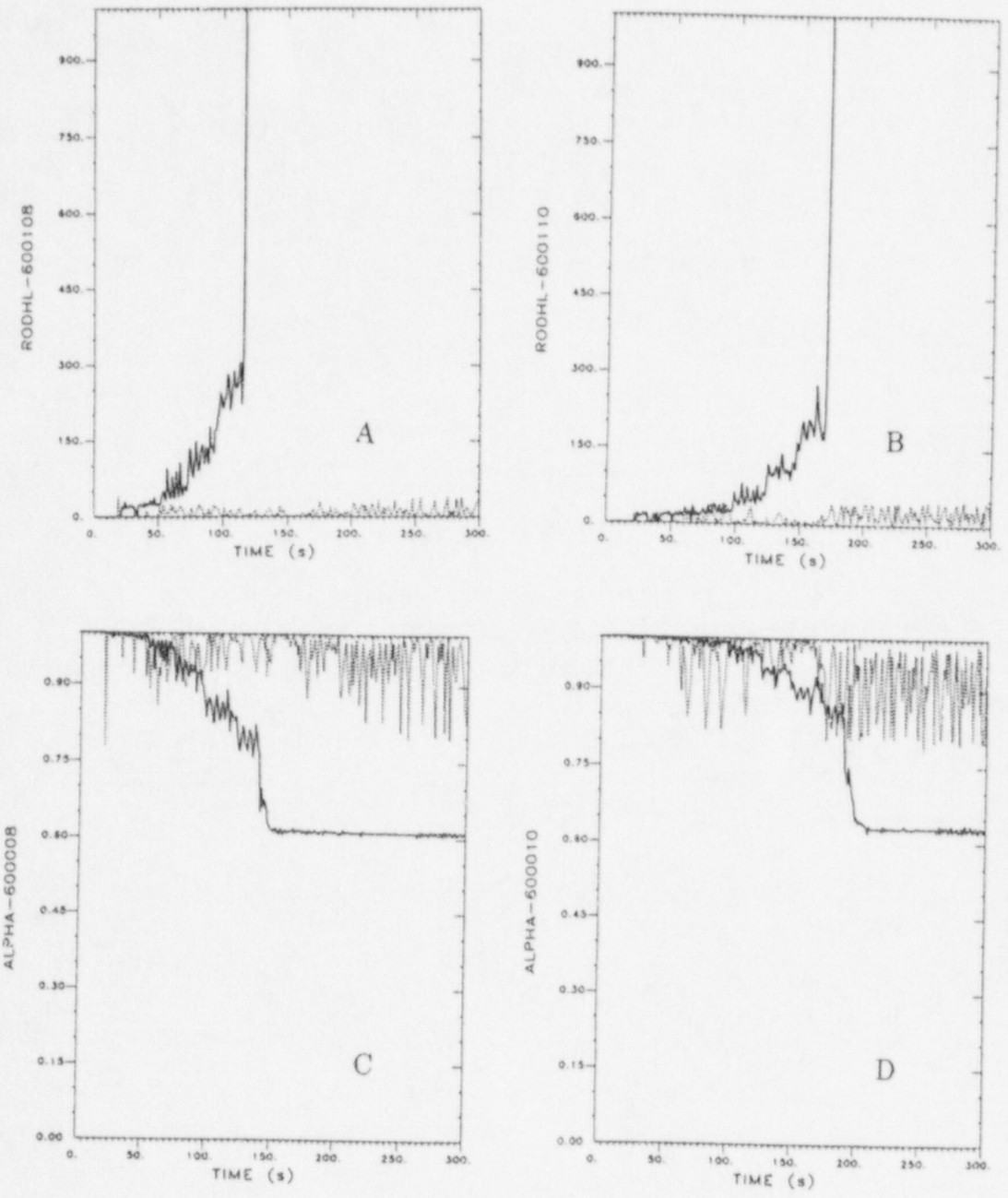

Fig.3 NEPTUN bottom flooding exp. Nr. 5036. HTC to the liquid ($W/m^2/K$) at axial elevations 0.714 m (A) and 0.946 m (B) and void fractions near the same elevations (C,D). (—): Modified TRAC-BF1; (.....): frozen version.

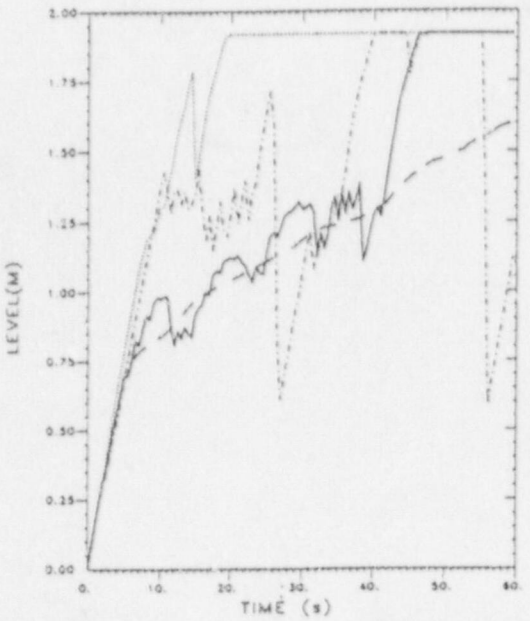

Fig.4 NEPTUN bottom flooding exp. Nr. 5050. Collapsed Liquid Level (m) . (—-): Modified TRAC-BF1; (.....): frozen version, ITMIN=0; (-.-.-): frozen version, ITMIN=1, (- - -): measurements.

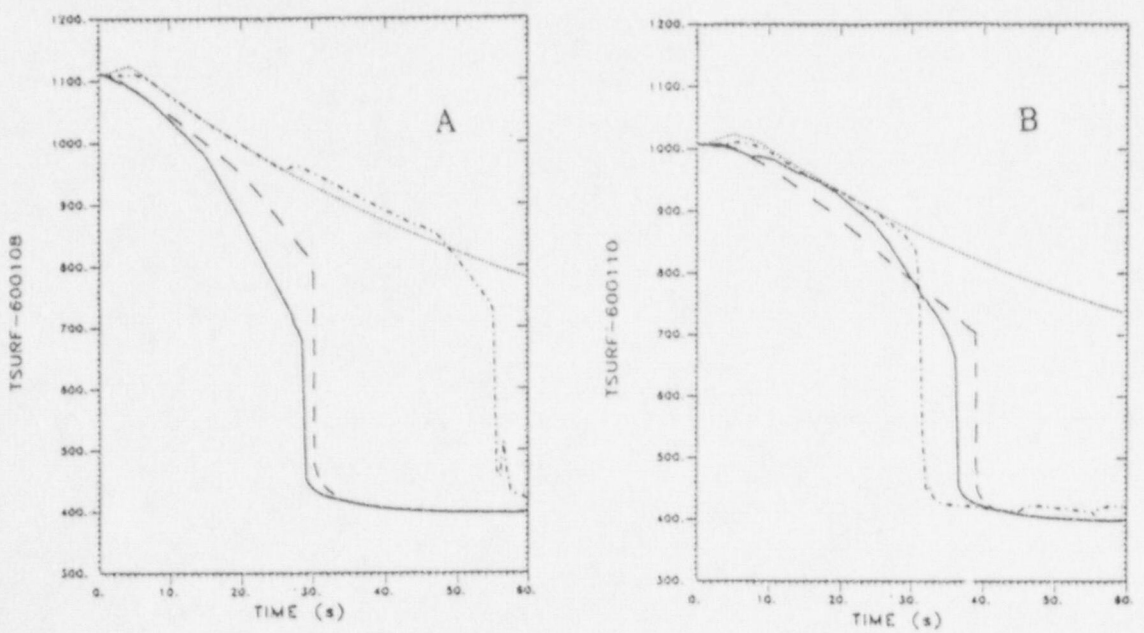

Fig.5 NEPTUN bottom flooding exp. Nr. 5050. RSTs (K) at axial elevations 0.714 m (A) and 0.946 m (B). (——): Modified TRAC-BF1; (.....): frozen version, ITMIN=0; (-.-.-): frozen version, ITMIN=1, (- - -): measurements.

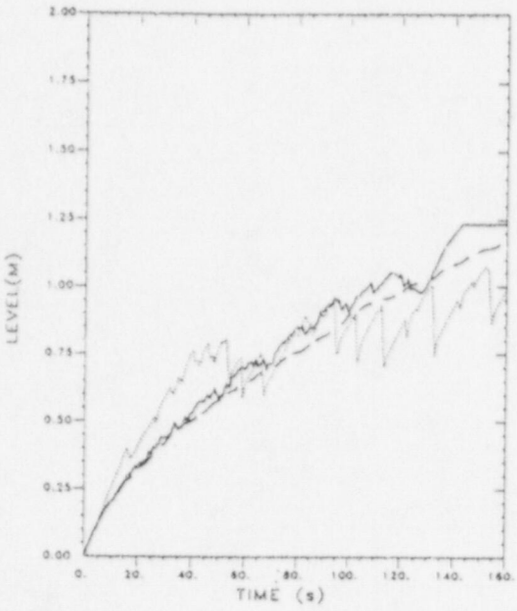

Fig.6 NEPTUN bottom flooding exp. Nr. 5052. Collapsed Liquid Level (m) (—): Modified TRAC-BF1; (.....): frozen version; (- - -): measurements.

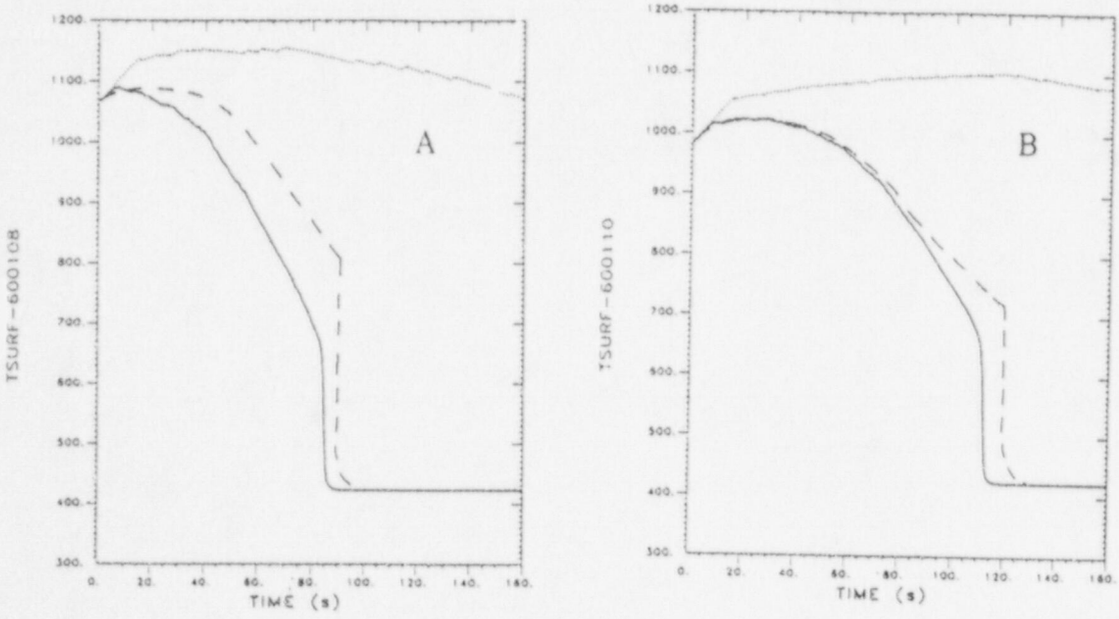

Fig.7 NEPTUN bottom flooding exp. Nr. 5052. RSTs (K) at axial elevations 0.714 m (A) and 0.946 m (B). (—): Modified TRAC-BF1; (.....): frozen version; (- - -): measurements.

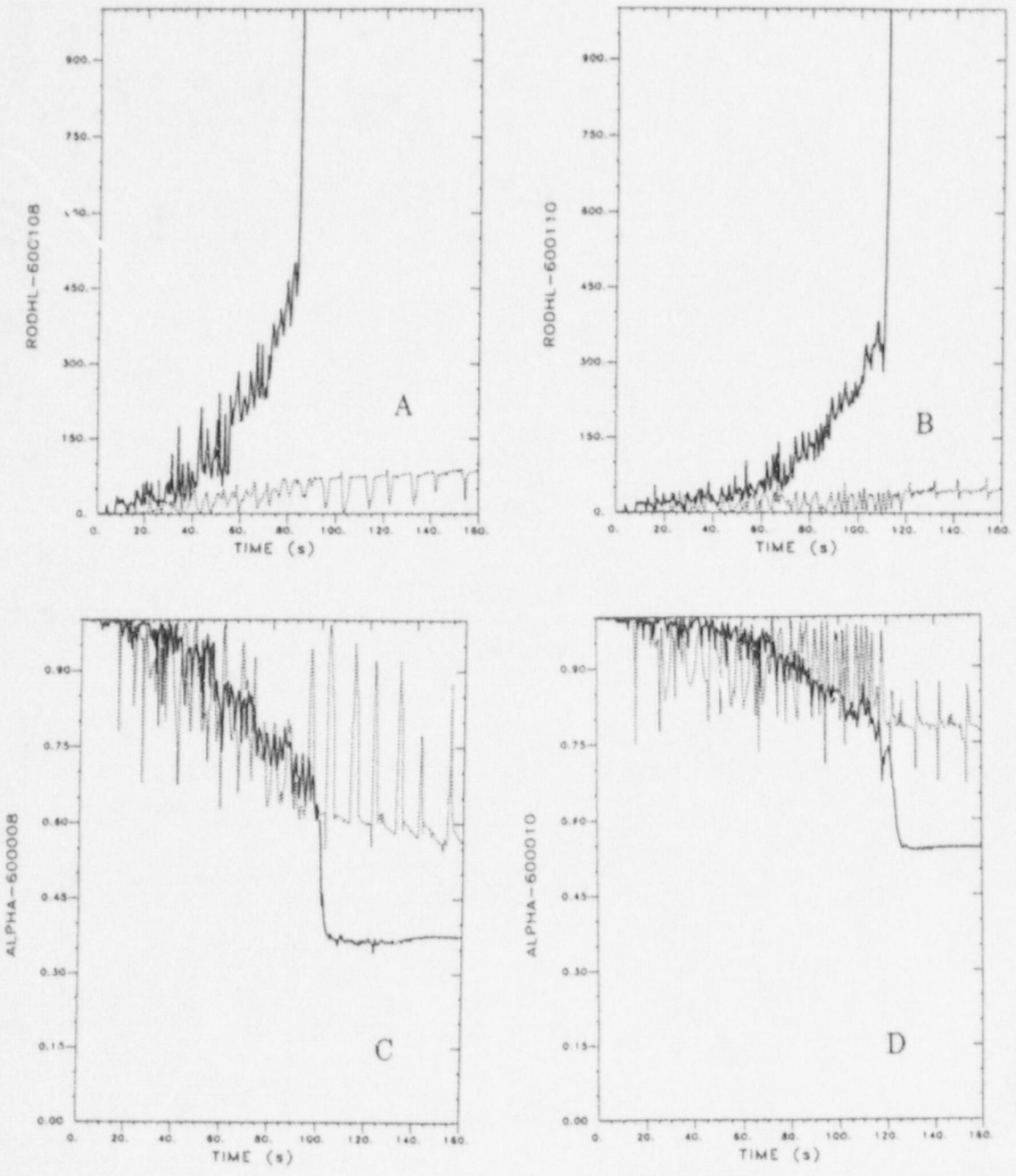

Fig.8 NEPTUN bottom flooding exp. Nr. 5052. HTC to the liquid ($W/m^2/K$) at axial elevations 0.714 m (A) and 0.946 m (B) and void fractions near the same elevations (C,D). (——): Modified TRAC-BF1; (.....): frozen version.

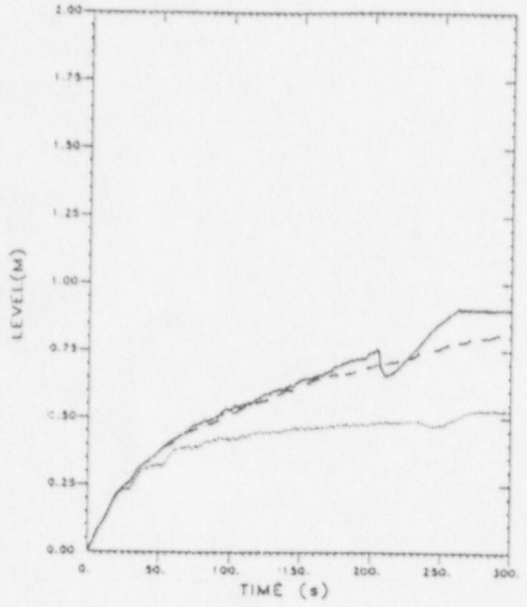

Fig.9 NEPTUN bottom flooding exp. Nr. 5036. Collapsed Liquid Level (m) . (——): Modified TRAC-BF1; (.....): Modified TRAC-BF1 with the annular flow interfacial shear of RELAP5/MOD2; (- - -): measurements.

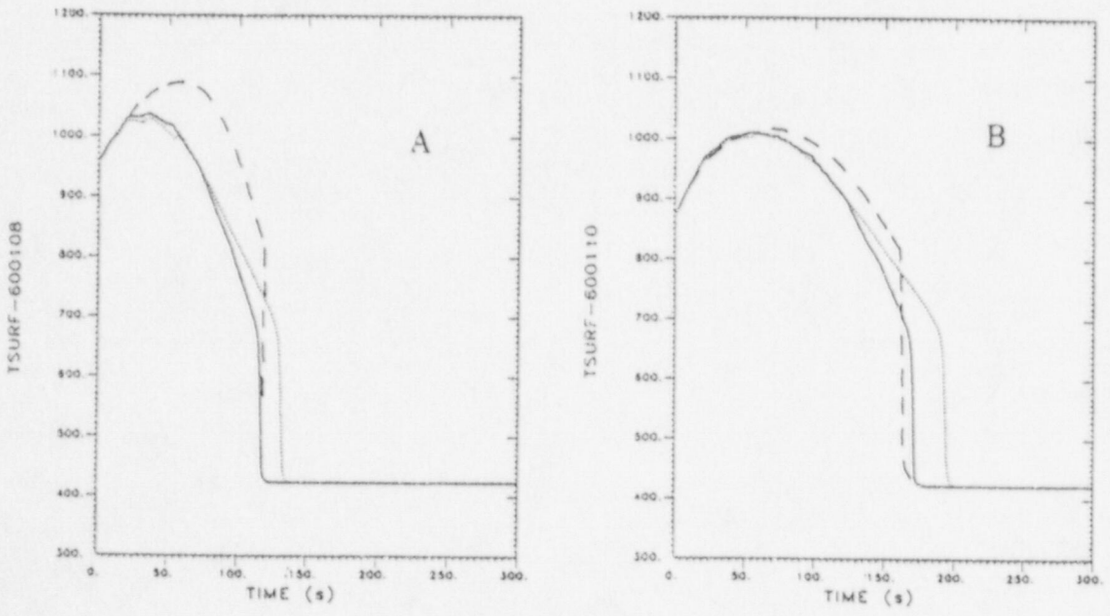

Fig.10 NEPTUN bottom flooding exp. Nr. 5036. RSTs (K) at axial elevations 0.714 m (A) and 0.946 m (B). (——): Modified TRAC-BF1; (.....): Modified TRAC-BF1 with the annular flow interfacial shear of RELAP5/MOD2; (- - -): measurements.

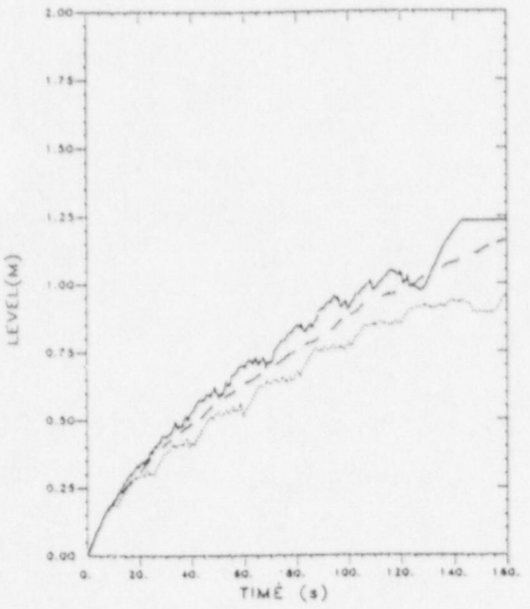

Fig.11 NEPTUN bottom flooding exp. Nr. 5052. Collapsed Liquid Level (m) . (——): Modified TRAC-BF1; (.....): Modified TRAC-BF1 with the annular flow interfacial shear of RELAP5/MOD2; (- - -): measurements.

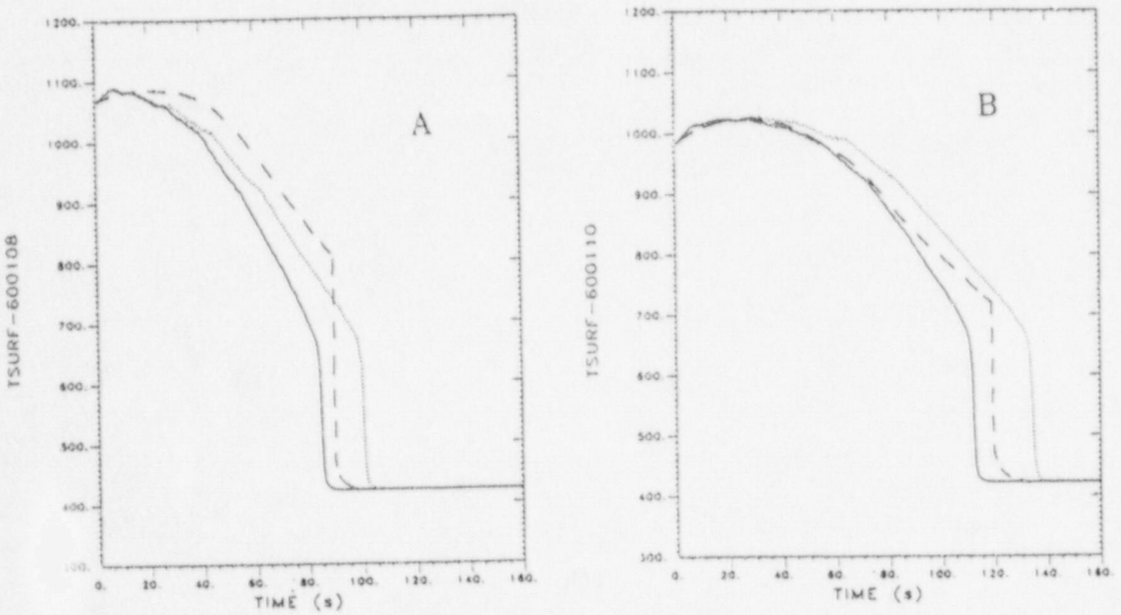

Fig.12 NEPTUN bottom flooding exp. Nr. 5052. RSTs (K) at axial elevations 0.714 m (A) and 0.946 m (B). (——): Modified TRAC-BF1; (.....): Modified TRAC-BF1 with the annular flow interfacial shear of RELAP5/MOD2; (- - -): measurements.

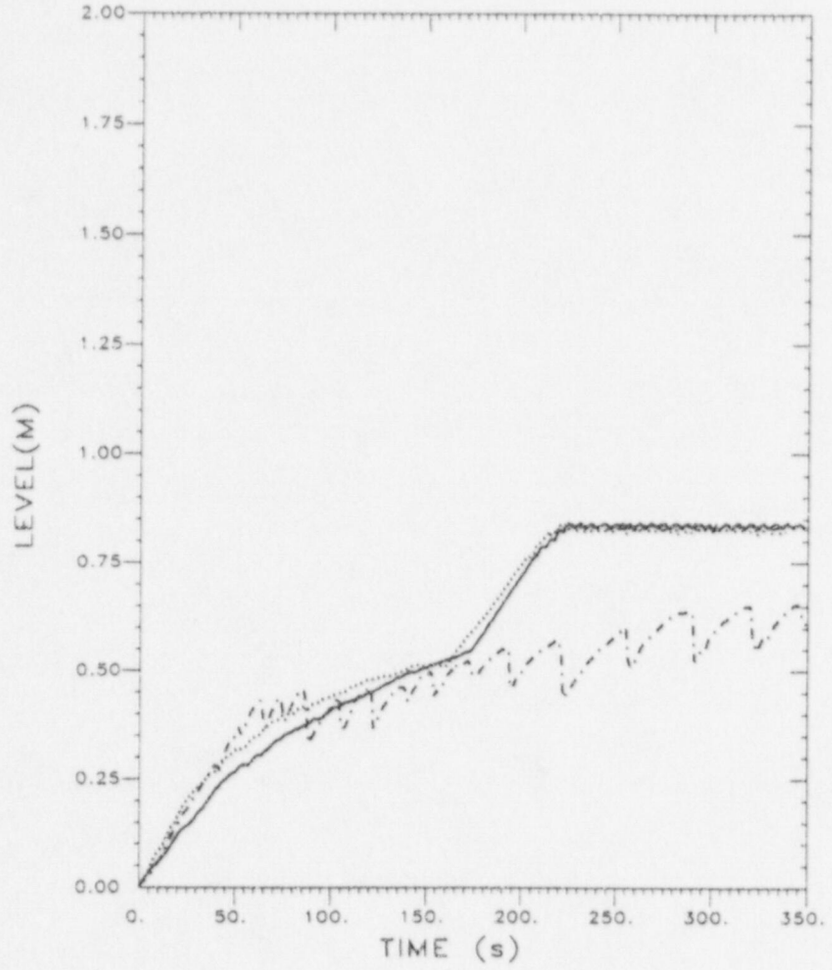

Fig.13 Benchmark top flooding test. Collapsed Liquid Level (m) . (——): Modified TRAC-BF1 with Wallis interfacial shear correlation and the annular flow wall shear of TRAC-PF1; (.....): Modified TRAC-BF1 with Wallis interfacial shear correlation; (-.-.-): frozen version.

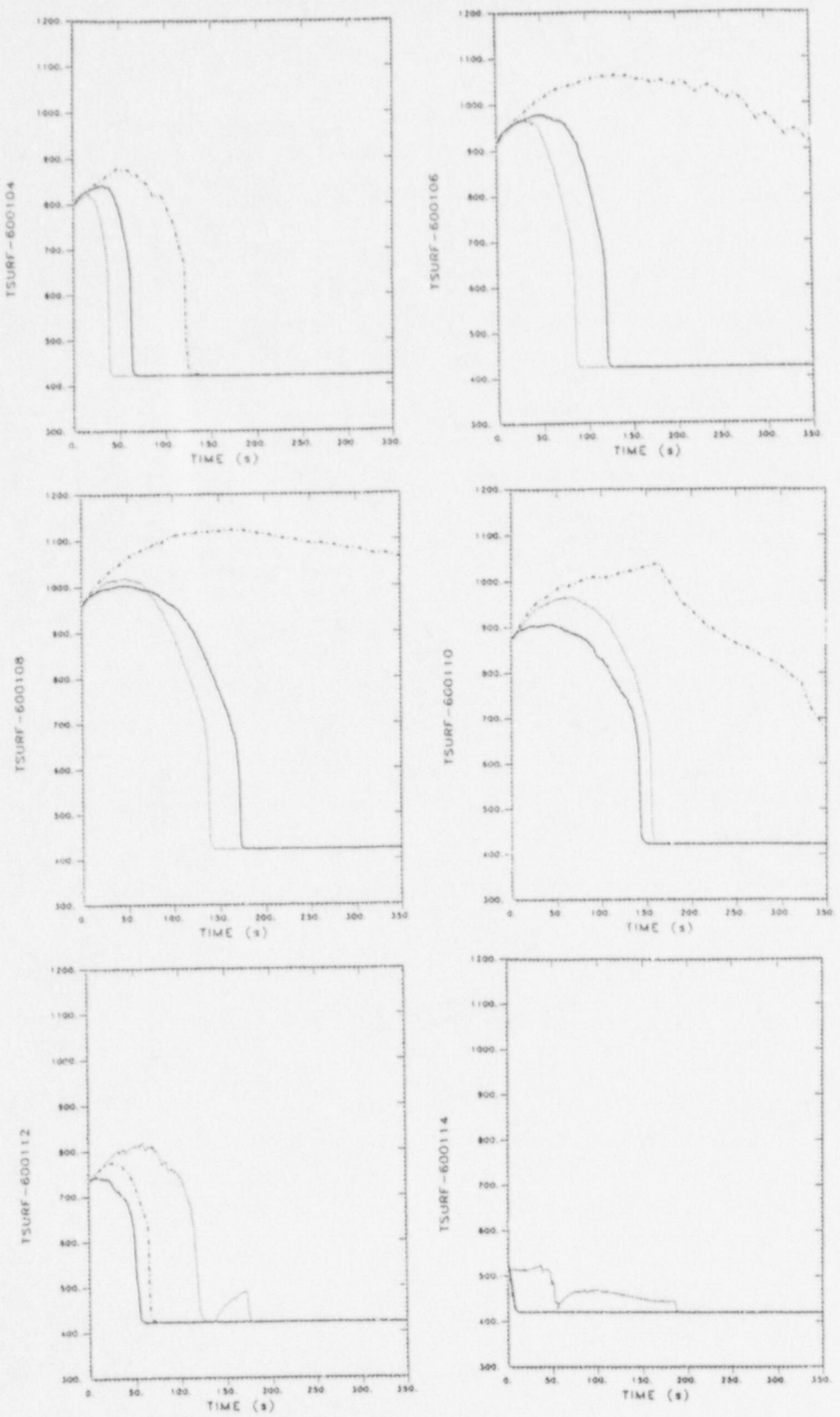

Fig.14 Benchmark top flooding test. RSTs (K) at 6 axial elevations. (——): Modified TRAC-BF1 with Wallis interfacial shear correlation and the annular flow wall shear of TRAC-PF1; (.....): Modified TRAC-BF1 with Wallis interfacial shear correlation; (-.-.-): frozen version.

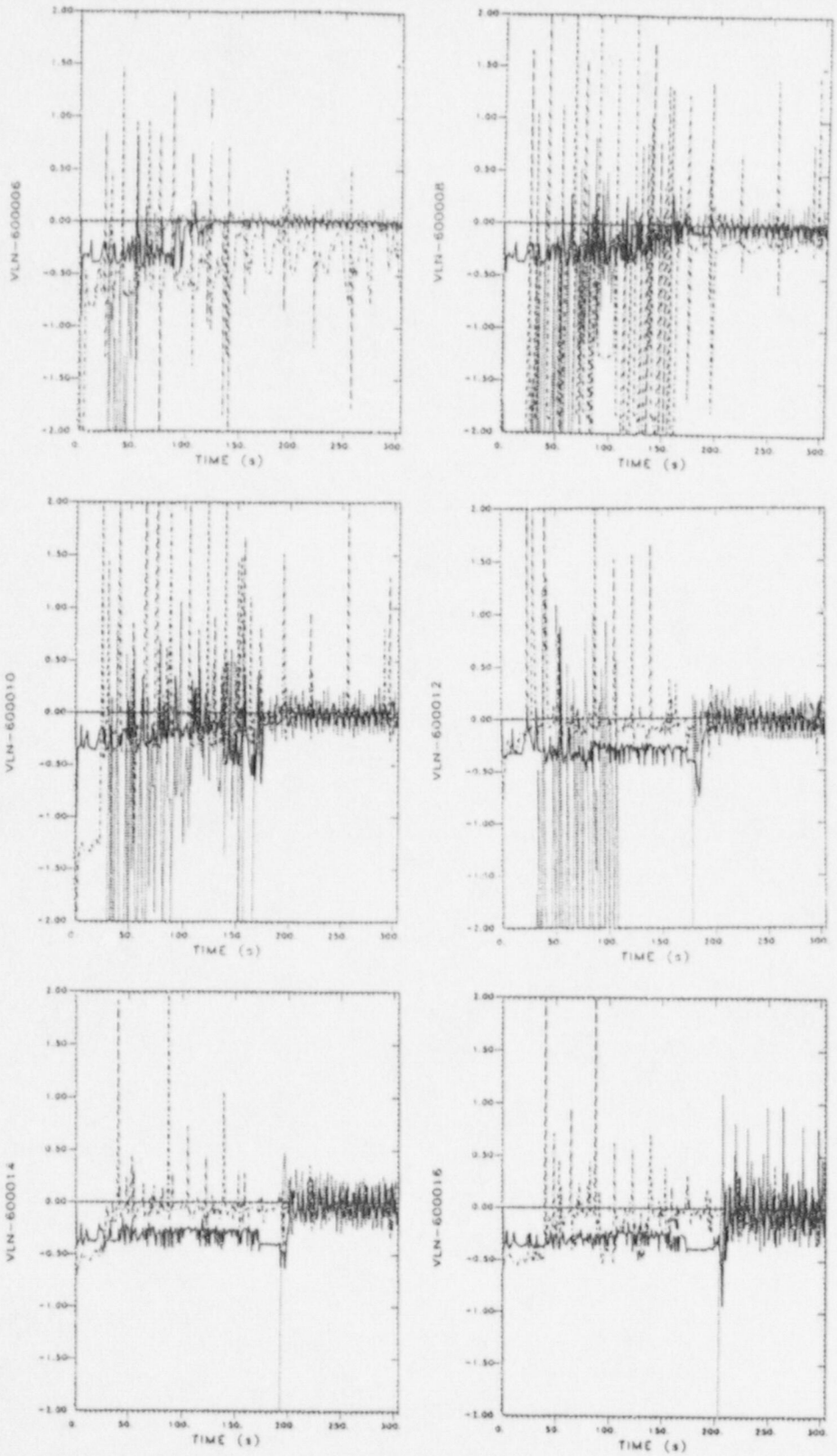

Fig.15 Benchmark top flooding test. Liquid velocities at 6 axial elevations. (——): Modified TRAC-BF1 with Wallis interfacial shear correlation and the annular flow wall shear of TRAC-PF1; (.....): Modified TRAC-BF1 with Wallis interfacial shear correlation; (-.-.-): frozen version.

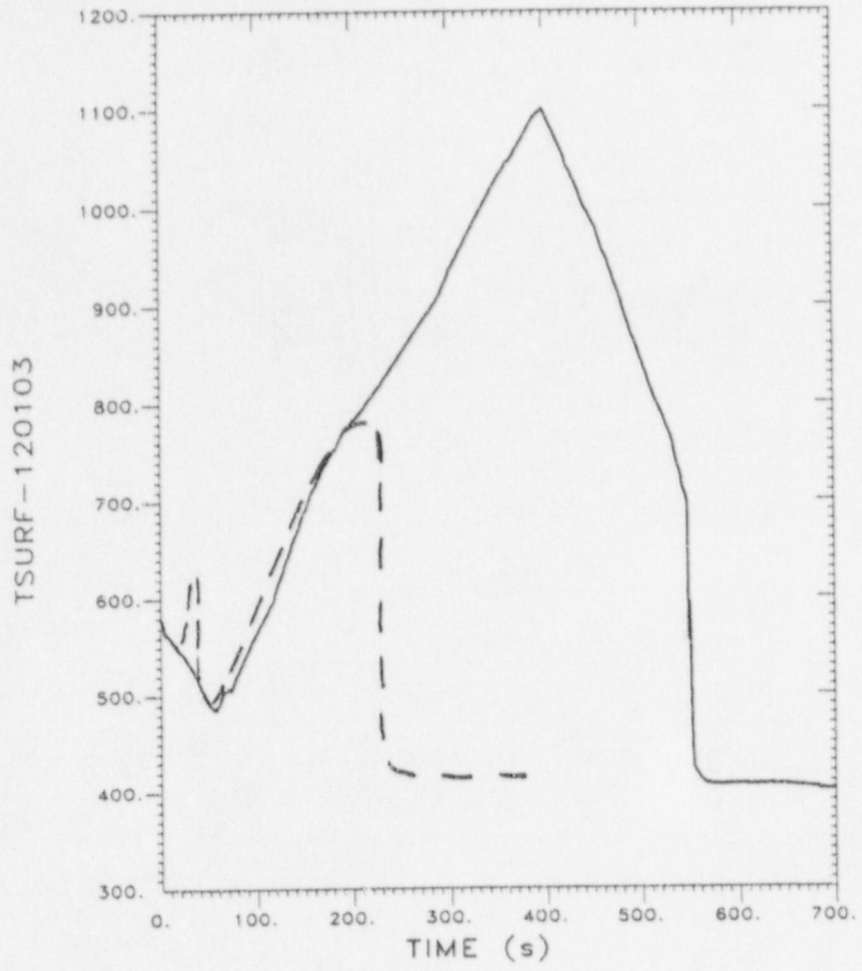

Fig.16 TLTA Test Nr. 6423. Comparison of measured (- - -) and predicted (——) "maximum" RST histories with the frozen version of the code and the fine-mesh activated during reflooding.

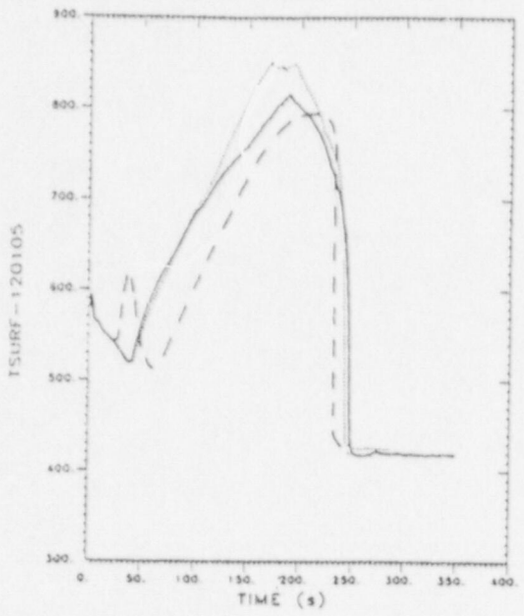

Fig.17 TLTA Test Nr. 6423. Comparison of measured (- - -) and predicted maximum RST histories. Andersen's annular flow shear model. (——): Modified TRAC-BF1; (.....): Modified TRAC-BF1 with upwinding option.

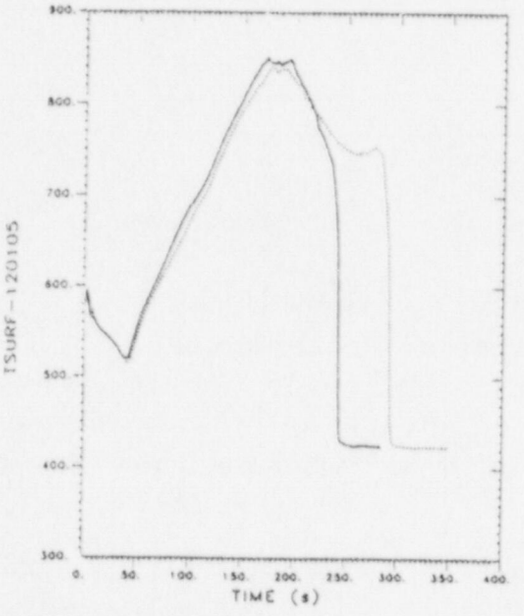

Fig.18 TLTA Test Nr. 6423. Comparison of predicted RST histories. Andersen's annular flow shear model. (——): Modified TRAC-BF1, upwinded both in 1D and 3D components; (.....): Modified TRAC-BF1 upwinded only in 1D components.

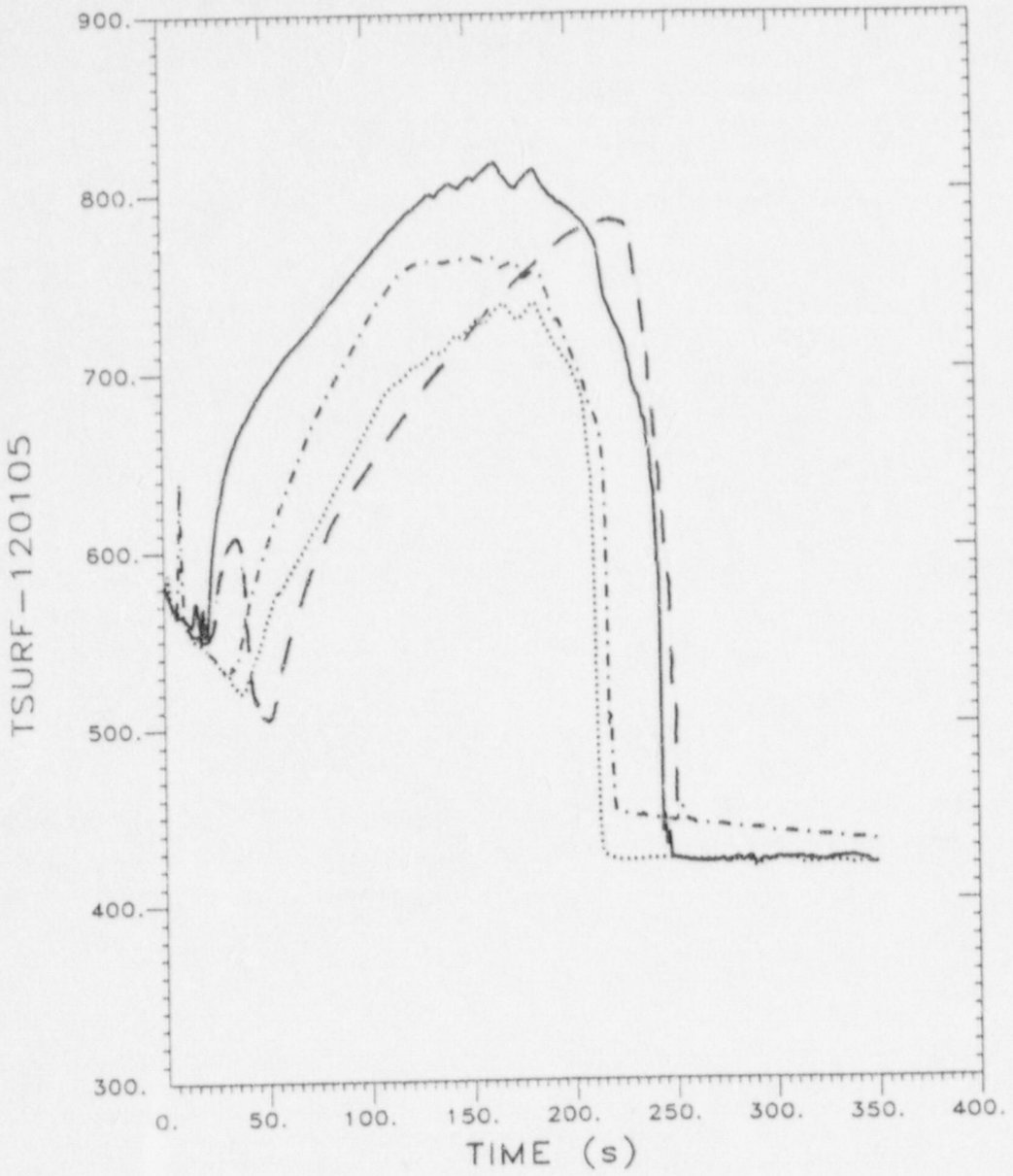

Fig.19 TLTA Test Nr. 6423. Comparison of measured (- - -) and predicted maximum RST histories with the Wallis annular flow interfacial shear correlation. (——): Modified TRAC-BF1 with homogeneous TRAC-PF1 wall shear model; (.....): Modified TRAC-BF1 with annular flow TRAC-PF1 wall shear model; (-.-.-): Modified TRAC-BF1 with no liquid fraction weighting of the wall shear to the liquid.

NRC FORM 335 (2-89) NRCM 1102, 3201, 3202

U.S. NUCLEAR REGULATORY COMMISSION

BIBLIOGRAPHIC DATA SHEET

(See instructions on the reverse)

1. REPORT NUMBER (Assigned by NRC, Add Vol., Supp., Rev., and Addendum Numbers, if any.)

NUREG/IA-0146

2. TITLE AND SUBTITLE

Implementation and Assessment of Improved Models and Options in TRAC-BF1

3. DATE REPORT PUBLISHED

MONTH	YEAR
October	1998

4. FIN OR GRANT NUMBER

W6667

5. AUTHOR(S)

G. Th. Analytis

6. TYPE OF REPORT

Technical

7. PERIOD COVERED (Inclusive Dates)

8. PERFORMING ORGANIZATION - NAME AND ADDRESS (If NRC, provide Division, Office or Region, U.S. Nuclear Regulatory Commission, and mailing address; if contractor, provide name and mailing address.)

Laboratory for Thermal Hydraulics
Paul Scherrer Institute
CH-5232 Villigen PSI
Switzerland

9. SPONSORING ORGANIZATION - NAME AND ADDRESS (If NRC, type "Same as above"; if contractor, provide NRC Division, Office or Region, U.S. Nuclear Regulatory Commission, and mailing address.)

Office of Nuclear Regulatory Research
Division of Systems Technology
U.S. Nuclear Regulatory Commission
Washington, DC 20555-0001

10. SUPPLEMENTARY NOTES

D.D. Ebert, NRC Project Manager

11. ABSTRACT (200 words or less)

A summary of modifications and options introduced in TRAC-BF1 is presented and is shown that the predicting capabilities of the modified version of the code are greatly improved. These changes include the introduction of a different heat transfer package during reflooding, the implementation of a simple single-phase limit procedure for forcing the two phases to acquire the same velocity if one phase disappears, a close assessment of the annular flow interfacial shear correlation, implementation of a simple radiation model which seems to alleviate some numerical-oscillation problems induced by the existing highly complex model. Furthermore, different options were introduced and tested like upwinding some terms of the momentum equations, the second upwind scheme for the convective terms of the phasic momentum equations and the implementation and assessment of a completely different annular flow interfacial shear correlation.

Modified TRAC-BF1 is assessed against some bottom-flooding separate-effect experiments, a "benchmark" top flooding simulation as well as against the TLTA test No. 6423. In the process of this task, the different options are assessed and discussed and is shown that the predictions of the modified code are physically sound and close to the measurements, while almost all the predicted variable are free of unphysical spurious oscillations. The modifications introduced solve a number of problems associated with the frozen version of the code and result in a version which can be confidently used for LBLOCA analyses.

12. KEY WORDS/DESCRIPTORS (List words or phrases that will assist researchers in locating the report.)

TRAC-BF1
LOCA
LBLOCA
reflood
TLTF
assessment
interfacial shear
radiation model

13. AVAILABILITY STATEMENT

unlimited

14. SECURITY CLASSIFICATION

(This Page) unclassified

(This Report) unclassified

15. NUMBER OF PAGES

16. PRICE

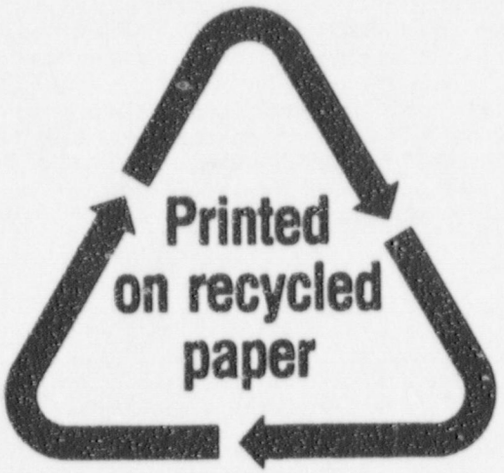

Federal Recycling Program